

Exact Verification of Graph Neural Networks with Incremental Constraint Solving

Minghao Liu, Chia-Hsuan Lu, and Marta Kwiatkowska

University of Oxford, United Kingdom
 {minghao.liu,chia-hsuan.lu,marta.kwiatkowska}@cs.ox.ac.uk

Abstract. Graph neural networks (GNNs) are increasingly employed in high-stakes applications, such as fraud detection or healthcare, but are susceptible to adversarial attacks. A number of techniques have been proposed to provide adversarial robustness guarantees, but support for commonly used aggregation functions in message-passing GNNs is lacking. In this paper, we develop an exact (sound and complete) verification method for GNNs to compute guarantees against attribute and structural perturbations that involve edge addition or deletion, subject to budget constraints. Our method employs constraint solving with bound tightening, and iteratively solves a sequence of relaxed constraint satisfaction problems while relying on incremental solving capabilities of solvers to improve efficiency. We implement GNNEV, a versatile exact verifier for message-passing neural networks, which supports three aggregation functions, sum, max and mean, with the latter two considered here for the first time. Extensive experimental evaluation of GNNEV on real-world fraud datasets (Amazon and Yelp) and biochemical datasets (MUTAG and ENZYMEs) demonstrates its usability and effectiveness, as well as superior performance for node classification and competitiveness on graph classification compared to existing exact verification tools on sum-aggregated GNNs.

Keywords: Formal verification · Constraint solving · Graph neural networks · Adversarial robustness

1 Introduction

Graph neural networks (GNNs) have been widely deployed in real-world applications, such as financial fraud detection [47, 65], autonomous driving [12, 13], healthcare treatment [25, 42], and scientific discovery [33, 52]. However, like all other neural network architectures, GNNs are vulnerable to adversarial attacks, where slight perturbations can cause a prediction change [19, 61, 80]. Therefore, it is desirable to ensure adversarial robustness of GNNs for high-stakes applications.

Formal verification is a rigorous methodology to mathematically prove that a system meets its specifications under all possible circumstances [17]. To evaluate the reliability and trustworthiness of neural networks, a number of approaches have been developed to verify the adversarial robustness of fully connected neural networks [9, 35, 66, 67, 74], convolutional neural networks (CNNs) [8, 32, 63], recurrent neural networks (RNNs) [1, 22, 37], and transformers [7, 60]. Technically, these approaches can be classified into two categories. The first category is *exact* verification, also known as *complete* verification, where the verification task is formulated as a constraint satisfaction problem (CSP) [54] to deterministically prove whether the model is robust or not. The second category is *approximate* verification, also known as (sound but) *incomplete* verification, where the non-convex constraints are typically relaxed to convex ones, which admits efficient computation of a lower bound on the robust region. However, when the lower bound cannot be accurately computed, the outcome of the verification may be inconclusive, which does not offer strong robustness guarantees.

Recently, the concept of adversarial robustness has been extended to GNNs. Graph inputs present additional challenges, in that the perturbations can pertain to both node attributes [2, 82] and graph structure, i.e., the addition and deletion of edges [5, 34, 38, 83], or even node injection [39]. Since graph inputs are encoded using a combination of real-valued and discrete data, typical approaches to provide *deterministic* robustness guarantees are based on Mixed-Integer Programming (MIP) [31, 75]. We also mention methods based on randomised smoothing [6, 50, 57], noting that their guarantees are *probabilistic* and thus not directly comparable.

Despite recent advances, existing exact verification approaches are still limited to GNNs with *sum* aggregation. However, other common aggregations, including *max* and *mean*, have been shown to be

necessary and effective in both theory [18, 53] and practice [21, 73], and are supported as standard by the GraphSAGE library [30]. Existing methods also typically focus on graph classification problems in the context of structural perturbations, implemented only for edge deletion for tractability reasons. Node classification tasks have been under-explored, and yet are relied upon in high-stakes applications, for example, fraud detection in financial networks [65] and cyber attack localization in smart grids [29]. For such applications, in order to provide certified robustness guarantees, methods that yield conclusive outcomes are preferable.

We develop an exact verification method for GNNs to provide guarantees against both attribute and structural perturbations subject to local and global budget constraints. We support GNNs for both node- and graph-classification tasks with three commonly used aggregation functions, sum, max and mean, where the latter two are non-linear. We employ constraint solving with bound tightening and iteratively solve a sequence of relaxed CSPs while relying on incremental solving capabilities of solvers to improve efficiency. We implement GNNEV, a versatile and efficient exact verifier for GNNs, and conduct extensive experiments on two standard node-classification datasets, Cora and CiteSeer, two real-world fraud datasets, Amazon and Yelp, and two biochemical graph-classification datasets, MUTAG and ENZYMEs. The results indicate that GNNEV outperforms SCIP-MPNN [31], the only MIP-based exact verifier known to us, on sum aggregation and edge deletion under different model sizes and perturbation budgets. On a range of aggregation functions, we show that GNNEV can provide useful insight into the susceptibility of GNNs to adversarial attacks, which is important for deployment in high-stakes applications.

Our novel contributions can be summarised as follows.

- We introduce the first exact verification method for GNNs with two common aggregation functions, max and mean, and design specialised tightened bound propagation strategies to reduce computational cost.
- We propose an algorithm that iteratively encodes GNN layers backwards and utilises incremental constraint solving to speed up performance while maintaining exact verification capability.
- We implement GNNEV, a versatile and efficient exact verifier for GNNs that supports new aggregation functions and edge addition, and show its usability on both structural and attribute perturbations through extensive experiments on real-world datasets.

2 Related Work

Verification of neural networks. Adversarial robustness verification methods can be classified into complete (exact) methods, such as constraint solving [32, 35, 62], or sound though incomplete methods, e.g., convex relaxation [55, 72], which can be strengthened to completeness by employing branch-and-bound procedures [11, 44]. Katz et al. [35] prove that exact NN verification is generally NP-hard. More recent works move beyond fully-connected and convolutional architectures, and include MIP-based exact verification of recurrent networks [1] and approximate verification of transformers utilising the zonotope abstract domain [7]. Regarding GNN verification, existing approaches concern graph convolutional networks with respect to attribute [2, 82] or structural [5, 34, 38, 83] perturbations. Most are approximate, relying on optimisation [5, 34, 38, 83] or zonotope-based relaxation [38]. Our approach is most similar to the exact MIP-based approach SCIP-MPNN [31] for sum-aggregated message-passing GNNs and edge deletion only. Their method supports static and dynamic (aggressive) bound tightening over the complete network encoding. In contrast, our method also supports max and mean, as well as edge addition, and proceeds by building the encoding incrementally layer by layer while statically tightening the bounds. For node classification tasks involving large numbers of neighbouring nodes, our exact method can greatly reduce the cost of encoding, thus enhancing performance. We also note a recent verifier ROBLIGHT [43], which supports structural perturbations only and references our work. Their method relies on a branch-and-bound approach with bound propagation, and is unable to generate certificates for verification that MIP-based methods permit [16].

Adversarial attacks against GNNs. Dai et al. [19], Xu et al. [70], Zügner et al. [80], Zügner and Günnemann [81] demonstrate that adversarial attacks can induce incorrect predictions by GNNs on node classification. Chang et al. [14], Mu et al. [48] propose black-box attack approaches without accessing any knowledge of the GNN classifiers. Li et al. [41], Zou et al. [79] further improve the efficiency

and scalability of adversarial attack algorithms. Another direction is attacks on graph classification [77] and link prediction [15, 78]. We emphasise that a failure to find an attack does not imply robustness. In contrast, we aim to verify that GNNs are not vulnerable to any admissible attack, which provides strong guarantees and can thus be used for robustness certification.

We further remark that, while most studies focus on undirected graphs and claim potential extensions to directed graphs, some works [15, 26], along with our paper, consider both directed and undirected graphs.

Robustness enhancement of GNNs. Adversarial training is a common technique applied to enhance the robustness of GNNs [20, 23, 28, 40, 70]. Wu et al. [68], Zhang and Zitnik [76] aim to enhance the robustness of GNNs by estimating and recovering potential adversarial perturbations. Moreover, generalised randomised smoothing [6, 64, 77] and partition-ensemble [69] techniques have been developed for GNNs to provide defences against attacks with probabilistic guarantees. Instead, we develop a formal verification algorithm, which is complementary to robustness enhancement and offers deterministic guarantees.

Theoretical analysis of GNN verification. Expressiveness of sum-aggregated GNNs is studied in Barceló et al. [3], Benedikt et al. [4], Nunn et al. [49] and mean-aggregated in Schönherr and Lutz [58]. The adversarial robustness problem for node classification is shown decidable in Sälzer and Lange [56] under the assumption of bounded degree of input graphs. Benedikt et al. [4] (and Nunn et al. [49]) study verification of certain properties that quantify over all graph inputs proving PSPACE-completeness for GNNs with rational (resp. integer) coefficients, Boolean-attributed input graphs and truncated ReLU activation functions. We focus instead on a practical verification approach applicable to commonly used GNNs, with real-valued coefficients and attributes and ReLU activation functions. Our problem setting is clearly decidable because it only considers a finite and bounded input graph set.

3 Preliminaries

3.1 Graph Neural Networks

Let $G = \langle V, E, X \rangle$ be an *attributed directed graph*, where $V = \{v_1, v_2, \dots, v_n\}$ is a set of nodes, $E \subseteq V \times V$ is a set of edges with no self-loops, and $X = \{\mathbf{x}_1, \mathbf{x}_2, \dots, \mathbf{x}_n\}$ is a set of real *attribute vectors* for the nodes with the same dimension. For a node $v \in V$ and a natural number k , we denote the set of k -hop incoming neighbours of v by $\mathcal{N}_k(v)$. For simplicity, we write $\mathcal{N}(v)$ when $k = 1$. *Graph neural networks (GNNs)* are a class of neural network architectures designed to operate on graph data. In this paper, we consider node- and graph-classification tasks. Given a class set $C = \{c_1, c_2, \dots, c_m\}$, for node classification, the goal is to classify a node $v \in V$ into a class within C ; for graph classification, the goal is to classify a graph G into a class within C . More precisely, we view a GNN as a function f such that, given an attributed directed graph $G = \langle V, E, X \rangle$ and a node $v \in V$, $f(G, v) \in C$ for node classification, and $f(G) \in C$ for graph classification. The remainder of the formalisation focuses on the node classification case for simplicity. The variant for graph classification is similar, as discussed in Appendix A.

There are a variety of GNN architectures. Existing formal verification works mostly focus on graph convolutional networks (GCNs) [36], which rely on a specific neighbourhood aggregation scheme and the expressiveness is restricted [71]. In this work, we consider *GraphSAGE* [30], also known as *Message-Passing Neural Networks (MPNNs)* [27], which are a more general GNN architecture because (i) they support the choice of multiple neighbourhood aggregation functions and (ii) the expressive power of MPNNs has been shown to encompass other popular variations such as GCNs and graph attention networks (GATs) [10].

A GNN consists of K layers. The dimension of a GNN is a $(K + 1)$ tuple of positive integers d_0, d_1, \dots, d_K . For an input attributed graph $G = \langle V, E, X \rangle$, for each node $v \in V$, its real-valued embedding vector $\mathbf{h}_v^{(0)}$ is a d_0 -dimension vector initialised to its corresponding attribute vector \mathbf{x}_v . For the k -th layer, GNNs compute the d_k -dimension embedding $\mathbf{h}_v^{(k)}$ by

$$\mathbf{h}_v^{(k)} = \sigma \left(\mathbf{W}_1^{(k)} \cdot \mathbf{h}_v^{(k-1)} + \mathbf{W}_2^{(k)} \cdot \text{aggr} \left(\left\{ \mathbf{h}_u^{(k-1)} \mid u \in \mathcal{N}(v) \right\} \right) + \mathbf{b}_1^{(k)} \right), \quad (1)$$

where $\mathbf{W}_1^{(k)}, \mathbf{W}_2^{(k)}$ are learnable parameter matrices with dimension $d_k \times d_{k-1}$ for the k -th layer, $\mathbf{b}_1^{(k)}$ is a learnable parameter vector, $\sigma(x) = \max(0, x)$ is the ReLU activation function, $\text{aggr} \in \{\text{sum}, \text{max}, \text{mean}\}$ is the aggregation function, and $\{\cdot\}$ denotes a multiset. Finally, the last dimension d_K is exactly m , and the predicted class \hat{c}_v of a node $v \in V$ is obtained by the Softmax function:

$$\hat{c}_v = \arg \max_{c \in C} \left(\text{Softmax} \left(\mathbf{h}_v^{(K)} \right) [c] \right). \quad (2)$$

3.2 Adversarial Robustness of GNNs

Node embeddings are directly affected by attribute perturbations and indirectly affected by structural perturbations through message passing, which may result in prediction instability. Changes in predictions caused by admissible perturbations indicate a lack of *adversarial robustness*. We adapt the definition of adversarial robustness for GNNs in Bojchevski and Günnemann [5] slightly by (i) allowing perturbations in both graph structure and node attributes, and (ii) removing the redundant fixed edge set. Given an attributed directed graph $G = \langle V, E, X \rangle$, the attacker typically has limited capabilities to perturb it. Let $F \subseteq V \times V$ be a set of *fragile edges*. Intuitively, an attacker can either remove edges in $F \cap E$ or insert edges in $F \setminus E$. For structural perturbations, we assume a global budget Δ and a local budget δ_v for each $v \in V$, both of which are non-negative integers. For attribute perturbations, we work with budgets $\epsilon_{v,i}^l, \epsilon_{v,i}^u$ ($\epsilon_{v,i}^l \leq \mathbf{x}_v[i] \leq \epsilon_{v,i}^u$) for each $v \in V$ and $i \in \{1, 2, \dots, d_0\}$, which are real values representing the range of perturbation allowed for the i -th dimension of $\mathbf{x}_v \in X$. The admissible perturbation space is defined as follows.

Definition 1 (Admissible perturbation space of graph). *Given an attributed directed graph $G = \langle V, E, X \rangle$, a set of fragile edges $F \subseteq V \times V$, and perturbation budgets Δ, δ, ϵ , the admissible perturbation space $\mathcal{Q}(G)$ of G with respect to F and budgets is the set of attributed directed graphs $\tilde{G} = \langle V, \tilde{E}, \tilde{X} \rangle$ that satisfy*

1. $E \setminus F \subseteq \tilde{E} \subseteq E \cup F$,
2. $|E \setminus \tilde{E}| + |\tilde{E} \setminus E| \leq \Delta$,
3. For every $v \in V$, $|\mathcal{N}(v) \setminus \tilde{\mathcal{N}}(v)| + |\tilde{\mathcal{N}}(v) \setminus \mathcal{N}(v)| \leq \delta_v$,
4. For every $v \in V$ and $1 \leq i \leq d_0$, $\epsilon_{v,i}^l \leq \tilde{\mathbf{x}}_v[i] \leq \epsilon_{v,i}^u$,

where we denote the incoming neighbours of v in the graph \tilde{G} by $\tilde{\mathcal{N}}(v)$. Note that this is a general formulation as F can be defined arbitrarily for different purposes, and allows us to consider edge addition when the size of F is moderate¹. For example, if $F = E$, only edge deletion is allowed, and any existing edge can be deleted. If $F = V \times V$, edges can be added or deleted between any pair of nodes.

Finally, we introduce the formal definition of adversarial robustness of GNNs.

Definition 2 (Adversarial robustness of GNNs). *Given a node-classification GNN f , an attributed directed graph G with admissible perturbation space $\mathcal{Q}(G)$, a target node $t \in V$, and its predicted class $\hat{c}_t \in C$, we say that f is adversarially robust for t with class \hat{c}_t if and only if, for every perturbed graph $\tilde{G} \in \mathcal{Q}(G)$, it holds that $f(\tilde{G}, t) = \hat{c}_t$.*

Adversarial robustness verification aims to guarantee that the prediction for a given node will not change under any admissible perturbations, subject to budget constraints, and can be reduced to computing the worst-case margin between the target class and other classes.

4 Exact Verification of GNNs

In this section, we introduce our method, which encodes the verification task as a constraint satisfaction problem (CSP). Next, the bound tightening strategies for max- and mean-aggregated GNNs are proposed. Finally, we illustrate an efficient exact verification algorithm based on incremental solving.

¹ The definition in Hojny et al. [31], Eq. (14) is a special case of ours when $F = E$.

4.1 Encoding

A CSP aims to determine whether there exists an assignment of variables that satisfies a given set of constraints. We encode the exact verification tasks as CSPs, which consist of three parts: input perturbation, GNN architecture, and verification objective. Following existing MIP encodings for GNNs [31, 75], we extend them to accommodate max and mean aggregations, where for mean we use big-M encoding and for max we rely on the solver.

Input perturbation. Consider an input graph $G = \langle V, E, X \rangle$, where our goal is to verify the adversarial robustness for the target node $t \in V$. Note that, for K -layer GNNs, only perturbations to nodes in $\mathcal{N}_K(t)$ can affect the prediction of t . Two kinds of perturbations are allowed. The first is attribute perturbation, where the node attributes can be modified within a specified range. For each node $v \in \mathcal{N}_K(t)$, we set d_0 real variables $attr_{v,1}, attr_{v,2}, \dots, attr_{v,d_0}$ as the attribute values after perturbations. Given the perturbation budgets $\epsilon_{v,i}^l, \epsilon_{v,i}^u$ for the i -th dimension of \mathbf{x}_v , the following constraint is applied:

$$\epsilon_{v,i}^l \leq attr_{v,i} \leq \epsilon_{v,i}^u. \quad (3)$$

The second type is structural perturbation, which can impact the message-passing mechanism. For each edge $(u, v) \in F$, we set a Boolean variable $pe_{u,v}$ to represent whether (u, v) is perturbed. Given the global budget Δ and the local budget δ_v for each $v \in \mathcal{N}_{K-1}(t)$, we have the constraints

$$\sum_{(u,v) \in F} pe_{u,v} \leq \Delta, \quad \sum_{(u,v) \in F} pe_{u,v} \leq \delta_v. \quad (4)$$

GNN architecture. We encode the architecture of GNNs as follows. For the k -th layer as shown in Eq. (1), the output embedding of node $v \in \mathcal{N}_{K-k}(t)$ is represented by d_k real variables $h_{v,1}^{(k)}, h_{v,2}^{(k)}, \dots, h_{v,d_k}^{(k)}$. Let $h_{v,i}^{(0)} = attr_{v,i}$. The encoding for each layer consists of three parts.

First, the neighbours of node v are aggregated to produce the message. We set d_{k-1} real variables $msg_{v,1}^{(k)}, msg_{v,2}^{(k)}, \dots, msg_{v,d_{k-1}}^{(k)}$ as the message vector. We support three common aggregation functions: sum, max, and mean. Note that the last two functions are non-linear, which accounts for higher computational complexity for verification. Before we give the encoding for the aggregation functions, we set the auxiliary variables $a_{v,i,u}^{(k)}$, which indicate the contribution of node u to $msg_{v,i}^{(k)}$ through the edge (u, v) . The following constraints restrict the values of $a_{v,i,u}^{(k)}$: for every $(u, v) \in E \setminus F$,

$$a_{v,i,u}^{(k)} = h_{v,i}^{(k-1)}; \quad (5)$$

for every $(u, v) \in E \cap F$,

$$pe_{u,v} \rightarrow a_{v,i,u}^{(k)} = 0 \quad \text{and} \quad \neg pe_{u,v} \rightarrow a_{v,i,u}^{(k)} = h_{v,i}^{(k-1)}; \quad (6)$$

for every $(u, v) \in F \setminus E$,

$$pe_{u,v} \rightarrow a_{v,i,u}^{(k)} = h_{v,i}^{(k-1)} \quad \text{and} \quad \neg pe_{u,v} \rightarrow a_{v,i,u}^{(k)} = 0. \quad (7)$$

For sum and max aggregation, the constraints are shown in Eq. (8) and (9), respectively.

$$msg_{v,i}^{(k)} = \sum_{(u,v) \in F \cup E} a_{v,i,u}^{(k)}, \quad (8)$$

$$msg_{v,i}^{(k)} = \max_{(u,v) \in F \cup E} a_{v,i,u}^{(k)}. \quad (9)$$

For mean aggregation, the constraints are set as follows:

$$\begin{aligned} deg_v &= \sum_{(u,v) \in F \cap E} (1 - pe_{u,v}) + \sum_{(u,v) \in F \setminus E} pe_{u,v} + |E \setminus F|, \\ deg_v \cdot msg_{v,i}^{(k)} &= \sum_{(u,v) \in F \cup E} a_{v,i,u}^{(k)}, \\ -M \cdot deg_v &\leq msg_{v,i}^{(k)} \leq M \cdot deg_v, \end{aligned} \quad (10)$$

where M is a big real number². Next, we introduce a constraint that represents the pre-ReLU embedding of node v as follows:

$$y_{v,i}^{(k)} = \sum_{j \in [1, d_{k-1}]} \mathbf{W}_1^{(k)}[i, j] \cdot h_{v,j}^{(k-1)} + \mathbf{W}_2^{(k)}[i, j] \cdot msg_{v,j}^{(k)} + \mathbf{b}_1^{(k)}. \quad (11)$$

Finally, we define the post-ReLU embedding, except the last GNN layer, as follows:

$$h_{v,i}^{(k)} = \max(y_{v,i}^{(k)}, 0). \quad (12)$$

Verification objective. According to Definition 2, our objective is to verify that no admissible attribute or structural perturbation can make the prediction of the GNN inconsistent with the input graph for a target node. Let the predicted class of target node t be \hat{c}_t , where the set of classes is denoted by C . Then we set the following constraint:

$$\left(\max_{c \in C \setminus \{\hat{c}_t\}} y_{t,c}^{(K)} \right) \geq y_{t,\hat{c}_t}^{(K)}, \quad (13)$$

which expresses the worst-case margin in the input of Softmax.

Let $\mathbf{y}_t^{(K)} = [y_{t,1}^{(K)}, y_{t,2}^{(K)}, \dots, y_{t,|C|}^{(K)}]$. Since the Softmax function is monotonically increasing, Eq. (13) implies that there exists $c \in C$ with $c \neq \hat{c}_t$ such that

$$\text{Softmax}(\mathbf{y}_t^{(K)})[c] \geq \text{Softmax}(\mathbf{y}_t^{(K)})[\hat{c}_t].$$

If Eq. (13) is feasible, this means that a perturbed graph has been found that makes the GNN misclassify node t . Therefore, the robustness verification task is translated to deciding whether the above CSP is unsatisfiable.

Note that the encoding involves at most $5N^2D$ real variables, N^2 Boolean variables, and $8ND + 2$ constraints, where N is the number of nodes in $\mathcal{N}_K(t)$ and $D := \sum_{0 \leq i \leq K} d_i$. Furthermore, the encoding can be computed in time polynomial in the size of the GNN.

4.2 Bound Tightening for Aggregations

Tightening of variable bounds has been found to be critical to enhancing the efficiency of MIP solvers. Simultaneously, high-quality bounds form the basis of our incremental solving algorithm introduced in Section 4.3. Starting from the input variables (i.e., $attr$), whose bounds have been determined by Eq. (3), we propagate these bounds layer by layer to obtain tight bounds for other variables.

Since tightened bound propagation is straightforward for linear transformations and ReLU functions, our main focus is on tightening the bounds for aggregation functions. We formalise the problem as follows: given three finite sets of variables X_1 , X_2 , and X_3 , the upper and lower bounds for each variable, and a non-negative integer s , compute the upper and lower bounds for the variable

$$z := \mathbf{aggr}(X_1 \cup X_2' \cup X_3'),$$

where $\mathbf{aggr} \in \{\text{sum, max, mean}\}$, $X_2' \subseteq X_2$, $X_3' \subseteq X_3$, and $|X_2 \setminus X_2'| + |X_3| \leq s$. Let N be the total size of the sets X_1 , X_2 , and X_3 . The intuition behind the formalisation is as follows: X_1 , X_2 , and X_3 represent the embedding vectors of nodes connected to the target node via non-fragile edges (E/F), fragile edges ($E \cap F$), and fragile non-edges (F/E), respectively. The attacker can either delete fragile edges, that is, remove elements from X_2 , or insert fragile non-edges, that is, select elements from X_3 . The number of deletion and insertions is constrained by the budget s .

For a set of variables X and an integer k , let $hi(X, k)$ denote the k -th *largest upper bound* among the variables in X . If $k > |X|$, we define $hi(X, k) = -\infty$. Similarly, let $lo(X, k)$ denote the k -th *smallest lower bound* among the variables in X , with $lo(X, k) = \infty$, if $k \leq 0$. Note that $hi(X, k)$ and $lo(X, k)$ can be computed in $O(|X| \log k)$ time by maintaining a max- or min-heap. For multiple values

² M is calculated by finding the maximum of the absolute values of the upper and lower bounds of all $a_{v,i,u}^{(k)}$ in Eq. (10).

k_1, k_2, \dots, k_ℓ , we can reuse the heap, resulting in an overall complexity of $O(|X| \log k)$, where k is the maximum value among k_1, k_2, \dots, k_ℓ .

For a variable x , its upper and lower bounds are denoted by \bar{x} and \underline{x} respectively. The case for sum aggregation has been shown by Hojny et al. [31]. We restate their bounds in the context of our formalisation for completeness:

$$\begin{aligned}\bar{z} &= \sum_{x \in X_1 \cup X_2} \bar{x} + \sum_{1 \leq i \leq s} \max(hi(Y, i), 0), \\ \underline{z} &= \sum_{x \in X_1 \cup X_2} \underline{x} + \sum_{1 \leq i \leq s} \min(lo(Y, i), 0),\end{aligned}$$

where $Y = \{-x \mid x \in X_2\} \cup X_3$. The upper and lower bounds of z can be computed in time $O(N \log s)$.

Max aggregation. The upper and lower bounds of z for the max aggregation can be obtained by case analysis. For the corner case $s = 0$, $z = \max(X_1 \cup X_2)$. Note that, if $X_1 \cup X_2 = \emptyset$, then $\bar{z} = \underline{z} = 0$. We now focus on the case $s > 0$. For the upper bound:

$$\bar{z} = \begin{cases} \max(0, hi(X_2, 1), hi(X_3, 1)), & \text{if } X_1 = \emptyset, s \geq |X_2|, \\ \max(hi(X_1, 1), hi(X_2, 1), hi(X_3, 1)), & \text{otherwise.} \end{cases}$$

On the other hand, for the lower bound:

$$\underline{z} = \begin{cases} \min(0, lo(X_2, 1), lo(X_3, 1)), & \text{if } X_1 = \emptyset, s > |X_2|, \\ \min(0, lo(X_2, 1)), & \text{if } X_1 = \emptyset, s = |X_2|, \\ lo(X_2, |X_2| - s), & \text{if } X_1 = \emptyset, s < |X_2|, \\ lo(X_1, |X_1|), & \text{if } X_1 \neq \emptyset, s \geq |X_2|, \\ \max(lo(X_1, |X_1|), lo(X_2, |X_2| - s)), & \text{if } X_1 \neq \emptyset, s < |X_2|. \end{cases}$$

Note that the upper and lower bounds for z can be computed in time $O(N \log s)$.

Mean aggregation. In this case, we reduce the original problem to a combination of subproblems. For non-negative integers s_2 and s_3 , define the variable

$$z_{s_2, s_3} := \mathbf{mean}(X_1 \cup X'_2 \cup X'_3),$$

where $X'_2 \subseteq X_2$, $X'_3 \subseteq X_3$, $|X_2 \setminus X'_2| = s_2$, and $|X'_3| = s_3$. The main difference is that we now explicitly fix separate budgets for deletions and insertions. The upper and lower bounds of the original problem z are given by

$$\bar{z} = \max_{\substack{s_2 + s_3 \leq s \\ 0 \leq s_2 \leq |X_2| \\ 0 \leq s_3 \leq |X_3|}} \bar{z}_{s_2, s_3} \quad \text{and} \quad \underline{z} = \min_{\substack{s_2 + s_3 \leq s \\ 0 \leq s_2 \leq |X_2| \\ 0 \leq s_3 \leq |X_3|}} \underline{z}_{s_2, s_3}.$$

For the subproblem z_{s_2, s_3} , since the budgets for deletion and insertion are separate, the upper and lower bounds can be obtained through greedy choices. In the corner case where X_1 is empty, $s_2 = |X_2|$, and $s_3 = 0$, $\bar{z}_{s_2, s_3} = \underline{z}_{s_2, s_3} = 0$. In all other cases, we have $\bar{z}_{s_2, s_3} = \bar{w}_{s_2, s_3}/n_{s_2, s_3}$ and $\underline{z}_{s_2, s_3} = \underline{w}_{s_2, s_3}/n_{s_2, s_3}$, where $n_{s_2, s_3} = |X_1| + |X_2| - s_2 + s_3$ and

$$\begin{aligned}\bar{w}_{s_2, s_3} &= \sum_{x \in X_1} \bar{x} + \sum_{1 \leq i \leq |X_2| - s_2} hi(X_2, i) + \sum_{1 \leq i \leq s_3} hi(X_3, i), \\ \underline{w}_{s_2, s_3} &= \sum_{x \in X_1} \underline{x} + \sum_{1 \leq i \leq |X_2| - s_2} lo(X_2, i) + \sum_{1 \leq i \leq s_3} lo(X_3, i).\end{aligned}$$

Note that the summations over lo and hi can be computed incrementally among subproblems and, as there are at most $(s + 1)^2$ subproblems, we can compute the upper and lower bounds for z in time $O(s^2 + N \log s)$ using a naïve approach. In fact, we can further improve this result by exploiting the unimodality of the sequence, reducing the computation time to $O((s + N) \log s)$. The detailed algorithm is provided in Appendix B.

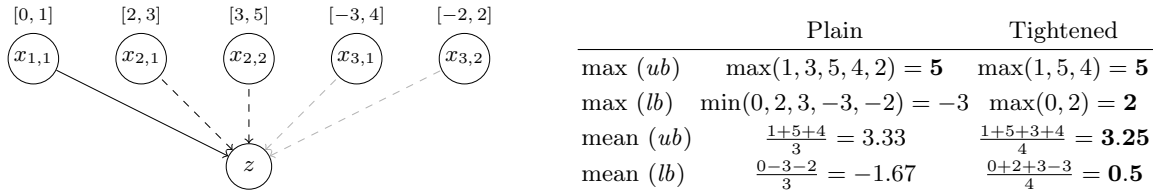


Fig. 1: An illustration of tightened bound propagation. Solid lines denote the non-fragile edges, black dashed lines denote fragile edges, and gray dashed lines denote fragile non-edges. The tighter bounds are shown in **bold**.

Theorem 1. *The upper and lower bounds provided in this section for max and mean aggregations are tight. That is, there exist sets $X'_2 \subseteq X_2$ and $X'_3 \subseteq X_3$ with $|X_2 \setminus X'_2| + |X_3 \setminus X'_3| \leq s$ that achieve these bounds exactly.*

The proof is included in Appendix C.

Example 1. Consider sets of variables $X_1 = \{x_{1,1}\}$, $X_2 = \{x_{2,1}, x_{2,2}\}$, and $X_3 = \{x_{3,1}, x_{3,2}\}$. Each variable has upper and lower bounds as shown in Fig. 1. Let the budget $s = 1$. We now consider tightened bound propagation:

- For max aggregation, the upper bound is 5 by no operation, the same as the plain method³; the lower bound is 2 by deleting $x_{2,2}$, improved by 5 over the plain method.
- For mean aggregation, the upper bound is 3.25 by inserting $x_{3,1}$, improved by 0.08; the lower bound is 0.5 by inserting $x_{3,1}$, improved by 2.17.

For both aggregations, tightened bound propagation reduces the domain of the variable z .

4.3 Verification with Incremental Solving

With tightened bound propagation, we can verify adversarial robustness of GNNs more efficiently. However, in node classification tasks, graphs are typically large in size, and for a node t we typically have that $|\mathcal{N}_{k+1}(t)| \gg |\mathcal{N}_k(t)|$ for the k -th layer, leading to rapid expansion of the encoding and a decrease in efficiency. To improve performance while maintaining exactness of verification, we utilise *incremental solving*, an effective mechanism in existing CSP solvers, to iteratively solve a series of simplified relaxation problems compared to the original problem.

Algorithm 1 describes our incremental solving-based verification method for GNNs. First, the CSP is formulated and the bounds of variables are derived based on the rules of bound tightening of Section 4.2 and layer-by-layer propagation (lines 1–6). Next, we solve the formula Φ iteratively using an incremental solving mechanism (lines 7–15). Initially, $\Phi = \varphi_{obj}$. For node classification, φ_{obj} only contains the variables representing the final embeddings of the target node t . For graph classification, φ_{obj} contains the variables representing the sum of final embeddings of all nodes, along with the final summation and linear transformation layer. In each iteration, new variables and the corresponding constraints are added to Φ , and a MIP solver S_Θ is then called (line 11), where Θ represents the generated cuts, which are redundant constraints produced by the solver to prune the search space. If Φ is found to be unsatisfiable, then the GNN has been verified to be **robust**. Otherwise, the encoding of the previous layer is added to Φ . Finally, if the result of the last iteration remains satisfiable, then the GNN is verified as **non-robust**. Note that, when each additional layer is added in the graph, the number of neighbouring nodes can increase significantly. Therefore, our algorithm effectively reduces the size of the encoding in early iterations, which leads to a more efficient exact verification process.

Finally, we show the correctness of Algorithm 1 with the proof in Appendix D:

Theorem 2. *Given a GNN f , an attributed directed graph G , and a perturbation space $\mathcal{Q}(G)$, f is adversarially robust (for a node t , if it is a node-classification GNN) if and only if Algorithm 1 returns **robust**.*

³ The plain method computes the upper (lower) bounds for max aggregation as the maximum (minimum) bound of all the variables, and for mean aggregation by sorting variable bounds from $X_2 \cup X_3$ in ascending order and finding the maximum (minimum) mean value among all postfix (prefix) sequences.

Algorithm 1 Exact Verification of GNNs with Incremental Solving

Input: Trained GNN f with K layers, attributed graph $G = \langle V, E, X \rangle$, target node t (for node classification), fragile edge set F , perturbation budgets Δ, δ, ϵ .

Output: Verification result.

```

1:  $Bounds \leftarrow \{attr, \overline{attr}\};$ 
2: for  $k$  from 1 to  $K$  do
3:    $\varphi_k \leftarrow \text{EncodeGNNLayer}(f, k, G, F, \Delta, \delta, \epsilon);$ 
4:    $Bounds \leftarrow \text{BoundPropagation}(\varphi_k, Bounds);$ 
5: end for
6:  $\varphi_{obj} \leftarrow \text{EncodeObjective}(\varphi_K, t);$  //Also encode final layer for graph classification.
7:  $S_\Theta \leftarrow \text{InitIncSolver}();$ 
8:  $\Phi \leftarrow \varphi_{obj};$ 
9: for  $k$  from  $K$  to 1 do
10:   $\Phi \leftarrow \Phi \wedge \varphi_k;$ 
11:   $result, \Theta \leftarrow \text{IncSolve}(S_\Theta, \Phi, Bounds);$ 
12:  if  $result = \text{unsat}$  then
13:    return robust;
14:  end if
15: end for
16: return non-robust;

```

5 Experimental Evaluation

5.1 Implementation and Setup

We implement our method as GNNEV, a versatile and efficient exact verifier specifically designed for message-passing GNNs⁴. GNNEV calls the underlying Gurobi 11.0.3 solver⁵ for MIP solving. Compared to available exact GNN verifiers, GNNEV has three advantages: (i) it accepts three commonly used aggregation functions, sum, max, and mean, which broadens usability, (ii) it allows for both node attribute perturbation and edge addition/deletion, making it applicable to a wider range of attack scenarios, and (iii) it is designed as a Python library that accepts trained models built by the SAGEConv module in PyTorch Geometric [24], and thus can be used directly in the same environment as model implementation and training.

To evaluate performance, we trained a batch of GraphSAGE models on two citation network datasets, Cora and CiteSeer [59], two real-world fraud datasets, Amazon [45] and Yelp [51], and two biochemical datasets, MUTAG and ENZYMES [46]. The first four datasets are for node classification and the last two are for graph classification. We set the number of GNN layers $K = 3$ and aggregation functions $\text{aggr} \in \{\text{mean}, \text{max}, \text{sum}\}$. We regard robustness verification for each node/graph as a task, which checks prediction stability for any set of admissible perturbations up to a given budget. For evaluation purposes, we run experiments with attribute and structural perturbation separately, but GNNEV supports their simultaneous use. All experiments were conducted on a server with Intel Xeon Gold 6252 @ 2.10GHz CPU, 252GB RAM, and Ubuntu 18.04 OS. A verifier, including both GNNEV and the baselines, ran each task on a single CPU core for fair comparison. The time limit for each task was set to 300s. More details of the datasets and experimental setups can be found in Appendix E.

5.2 Comparison with Baselines on Sum-aggregation

We compare GNNEV to SCIP-MPNN [31] on edge deletion⁶, the only MIP-based exact verifier immediately applicable to adversarial robustness of GNNs⁷. SCIP-MPNN includes five variants with different underlying solvers and bound tightening strategies. To make fair comparison, we use the two

⁴ The source code and data will be made publicly available in the final version.

⁵ <https://www.gurobi.com>

⁶ We note that SCIP-MPNN does not implement edge addition and its interface does not support attribute perturbations.

⁷ We remark that ROBLIGHT outperforms our tool but it is not MIP-based, limited to structural perturbations only and does not allow certificate generation as described in Section 1.

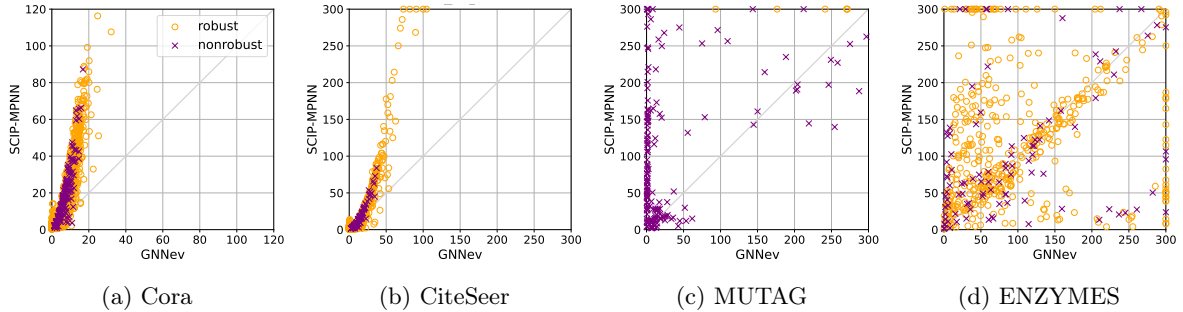


Fig. 2: Comparison of runtime (in seconds) for sum-aggregated GNNs on node classification (a-b) and graph classification (c-d). Each data point represents a robustness verification task with $\Delta = 2$. A point above the diagonal line indicates that GNNEV outperforms SCIP-MPNN on that task.

versions that also call Gurobi: GRBbasic and GRBsbt⁸. For each task, we ran these two versions separately and reported the shorter runtime as the result of SCIP-MPNN. To align with the restrictions of SCIP-MPNN, we utilised GNNs with sum aggregation, only allowed edge deletions (i.e., $F = E$), and adapted our verification objective⁹.

Results. Fig. 2 demonstrates the comparison of runtime between GNNEV and SCIP-MPNN with edge deletions. For node-classification datasets, Cora and CiteSeer, GNNEV solved all tasks within 40s and 120s, respectively, outperforming SCIP-MPNN on the vast majority of tasks. Note that GNNEV also solved 5 challenging tasks on which SCIP-MPNN failed within the time limit on CiteSeer. For graph-classification datasets, GNNEV demonstrated competitive performance. On MUTAG, GNNEV solved most tasks within seconds, likely due to the simpler and more efficient encoding produced through incremental solving. On ENZYMES, a highly challenging dataset, GNNEV also performed well compared to SCIP-MPNN by completing 6.1% of the solvable tasks that SCIP-MPNN could not complete within the time limit, and reducing runtime on 54.8% of the solvable tasks. Our experiments thus indicate that GNNEV is a highly promising approach for exact verification. See Appendix F for detailed comparison results on different perturbation budgets.

5.3 Performance on All Aggregation Functions

Next, we systematically evaluated the performance of GNNEV on sum-, max- and mean-aggregated GNNs with structural perturbations. For this experiment we set the strong verification objective as Eq. (13), which is more challenging to compute than Hojny et al. [31], Eq. (11). Due to the large number of nodes in Amazon and Yelp, we randomly selected 1,000 nodes for verification. Two fragile edge sets F were used: (i) *edge deletions* are allowed for all edges, i.e., $F = E$, and (ii) *edge additions* are allowed for selected set, i.e., for each node v , several sampled non-edges $(u, v) \notin E$ are added to F . See Appendix F for more details.

Results. Fig. 3 illustrates the runtime of GNNEV on real-world node- and graph-classification datasets under different aggregations and budgets Δ for edge deletion; results on additional datasets and for edge addition are in Fig. 5,6 in Appendix F. First, MUTAG and ENZYMES are more challenging, as incremental solving can reduce the number of variables representing both nodes and layers for node classification, whereas it can only reduce the number of variables representing layers for graph classification. Second, across different aggregations, there was a performance drop for max aggregation when $\Delta \geq 5$, likely due to Gurobi struggling to efficiently process max constraints using internal big-M

⁸ We excluded the three variants based on SCIP, noting that the experimental results in Hojny et al. [31] showed that GRBbasic and GRBsbt have notably shorter runtime.

⁹ According to Hojny et al. [31], Eq. (11) and Section 4.2, given the predicted class \hat{c}_t for target node t , SCIP-MPNN aims to verify that $\mathbf{h}_t^{(K)}[\hat{c}_t] > \mathbf{h}_t^{(K)}[(\hat{c}_t + 1)\%|C|]$ holds for all perturbed graphs. This simpler objective, which provides weaker robustness guarantees than ours stated in Eq. (14), is used for tractability reasons.

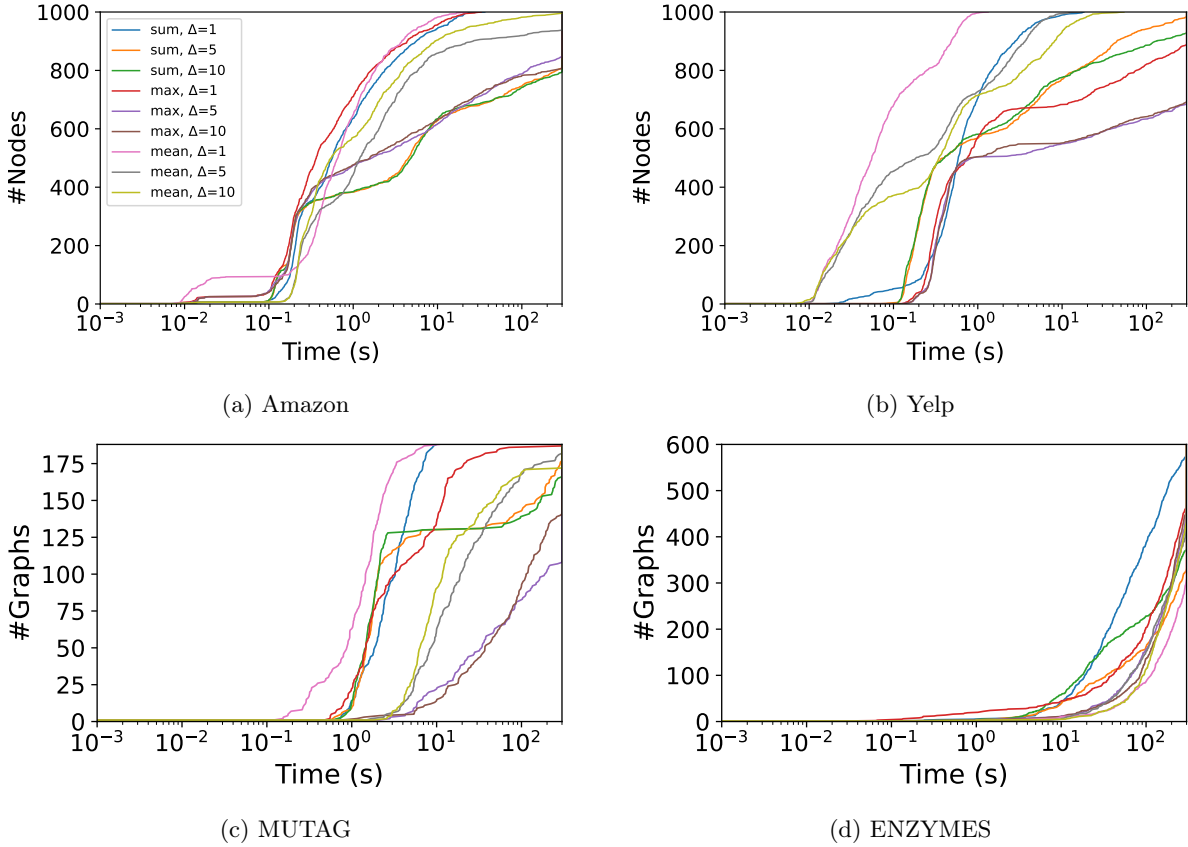


Fig. 3: The number of tasks solved by GNNEV on real-world node-classification (a-b) and graph-classification (c-d) datasets plotted against runtime under different aggregations and budgets. Only edge deletions are allowed ($F = E$). The verification objective is as defined in Section 4.1, Eq. (13). Full results are shown in Fig. 5 in Appendix F.

encoding. Moreover, for sum aggregation, the performance on Amazon and Yelp dropped compared to Cora and CiteSeer. This can be attributed to the much larger gap between upper and lower bounds of variables, which is most pronounced for sum aggregation in Table 5 in Appendix F, where we see a significant increase in the gap after each layer. Finally, we conducted ablation experiments to show the effectiveness of bound tightening and incremental solving, with results detailed in Appendix F.

5.4 Adversarial Robustness Case Study

We further use GNNEV to analyse the robustness of GNNs for both structural and attribute perturbations, especially in high-stakes domains such as fraud detection and scientific discovery. First, we performed evaluation of the number of (non-)robust tasks verified plotted against an increasing global structural perturbation budget, shown in Fig. 7,8 in Appendix F. In most cases, instances were attacked successfully with a small budget. Some GNNs exhibited quite weak robustness. Specifically, we found that mean-aggregated GNNs were more vulnerable to adversarial perturbations than other types. Moreover, GNNEV was executed on Amazon and Yelp to verify mean-aggregated GNNs with attribute perturbation enabled. From the results shown in Fig. 9 in Appendix F, even perturbing a single dimension of attributes can cause models to make wrong predictions in up to 75.8% of tasks.

Within these results, we identified a number of adversarial attacks on non-robust instances, which demonstrate the vulnerability of GNNs. Fig. 4 illustrates two cases from Amazon and MUTAG, respectively. In Amazon, one of the attributes is the length of username, which is easily manipulated in practice. We configured GNNEV to only allow perturbations of this attribute within the range $[1, 10]$. The results showed that 29.1% of nodes were successfully attacked for the mean-aggregated GNN. In MUTAG, edge addition and deletion can easily lead to invalid structures, but GNNEV found that

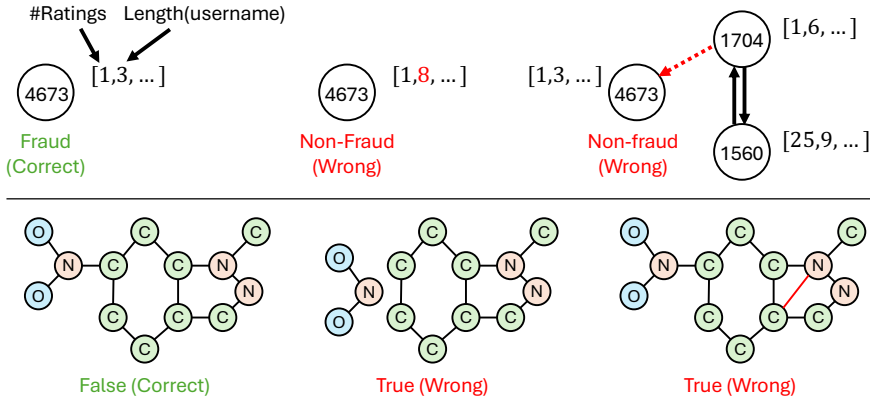


Fig. 4: Adversarial examples found by GNNEV. Top: Either modifying an attribute (here length of username) or adding an edge caused a node in the Amazon dataset to be misclassified as non-fraudulent. Bottom: Adding or deleting an edge on a graph in the MUTAG dataset leads to wrong prediction of having the given property even if the perturbed graphs are invalid.

mean-aggregated GNNs reported 12.7% false positive results when $\Delta = 1$. These demonstrate that GNNEV is able to gain useful insight into the susceptibility of GNN models to adversarial attacks, which is important for pre-deployment analysis for high-stakes applications.

6 Conclusion and Future Work

We have developed an exact robustness verification method for message-passing GNNs supporting a range of aggregation functions, which is implemented in GNNEV, a versatile and efficient verifier. Our approach is based on a reduction to a constraint satisfaction problem with bound tightening, solved incrementally. The support for two common aggregation functions, max and mean, is formulated here for the first time. Experiments on a range of datasets show that GNNEV can verify adversarial robustness of GNNs to attribute and structural perturbations. It outperforms state-of-the-art MIP-based baselines on node classification in both efficiency and functionality while remaining competitive on graph classification, and delivers strong performance on real-world fraud and biochemical datasets. One practical limitation of our approach is that the computational complexity grows quickly with the size of the fragile edge set. Future work will include mitigating the impact of the fragile edge sets on performance by combining heuristic search and distributed frameworks.

Acknowledgments. The authors would like to thank Michael Benedikt for the insightful comments and suggestions. This work was supported by the EPSRC Prosperity Partnership FAIR (grant number EP/V056883/1) and ELSA: European Lighthouse on Secure and Safe AI project (grant agreement No. 101070617 under UK guarantee). MK receives funding from the ERC under the European Union’s Horizon 2020 research and innovation programme (FUN2MODEL, grant agreement No. 834115).

References

1. Akintunde, M.E., Kevorchian, A., Lomuscio, A., Pirovano, E.: Verification of RNN-based neural agent-environment systems. In: AAAI 2019, pp. 6006–6013 (2019)
2. An, D., Zhang, H., Zhao, Q., Liu, J., Shi, J., Huang, Y., Yang, Y., Liu, X., Qin, S.: Graph convolutional network robustness verification algorithm based on dual approximation. In: ICFEM 2024, pp. 146–161 (2024)
3. Barceló, P., Kostylev, E.V., Monet, M., Pérez, J., Reutter, J.L., Silva, J.P.: The Logical Expressiveness of Graph Neural Networks. In: ICLR (2020)
4. Benedikt, M., Lu, C., Motik, B., Tan, T.: Decidability of graph neural networks via logical characterizations. In: ICALP 2024, pp. 127:1–127:20 (2024)
5. Bojchevski, A., Günnemann, S.: Certifiable robustness to graph perturbations. In: NeurIPS 2019, pp. 8317–8328 (2019)

6. Bojchevski, A., Klicpera, J., Günnemann, S.: Efficient robustness certificates for discrete data: Sparsity-aware randomized smoothing for graphs, images and more. In: ICML 2020, pp. 1003–1013 (2020)
7. Bonaert, G., Dimitrov, D.I., Baader, M., Vechev, M.T.: Fast and precise certification of transformers. In: PLDI 2021, pp. 466–481 (2021)
8. Boopathy, A., Weng, T., Chen, P., Liu, S., Daniel, L.: CNN-Cert: An efficient framework for certifying robustness of convolutional neural networks. In: AAAI 2019, pp. 3240–3247 (2019)
9. Botoeva, E., Kouvaros, P., Kronqvist, J., Lomuscio, A., Misener, R.: Efficient verification of relu-based neural networks via dependency analysis. In: AAAI 2020, pp. 3291–3299 (2020)
10. Bronstein, M.M., Bruna, J., Cohen, T., Velickovic, P.: Geometric deep learning: Grids, groups, graphs, geodesics, and gauges. *CoRR* **abs/2104.13478** (2021)
11. Bunel, R., Turkaslan, I., Torr, P.H.S., Kohli, P., Mudigonda, P.K.: A unified view of piecewise linear neural network verification. In: NeurIPS 2018, pp. 4795–4804 (2018)
12. Cai, P., Wang, H., Sun, Y., Liu, M.: DiGNet: Learning scalable self-driving policies for generic traffic scenarios with graph neural networks. In: IROS 2021, pp. 8979–8984 (2021)
13. Casas, S., Gulino, C., Liao, R., Urtasun, R.: SpAGNN: Spatially-aware graph neural networks for relational behavior forecasting from sensor data. In: ICRA 2020, pp. 9491–9497 (2020)
14. Chang, H., Rong, Y., Xu, T., Huang, W., Zhang, H., Cui, P., Zhu, W., Huang, J.: A restricted black-box adversarial framework towards attacking graph embedding models. In: AAAI 2020, pp. 3389–3396 (2020)
15. Chen, J., Zhang, J., Chen, Z., Du, M., Xuan, Q.: Time-aware gradient attack on dynamic network link prediction. *IEEE Trans. Knowl. Data Eng.* **35**(2), 2091–2102 (2023)
16. Cheung, K.K.H., Gleixner, A.M., Steffy, D.E.: Verifying integer programming results. In: IPCO 2017, pp. 148–160 (2017)
17. Clarke, E.M., Wing, J.M.: Formal methods: State of the art and future directions. *ACM Comput. Surv.* **28**(4), 626–643 (1996)
18. Corso, G., Cavalleri, L., Beaini, D., Liò, P., Velickovic, P.: Principal neighbourhood aggregation for graph nets. In: NeurIPS 2020 (2020)
19. Dai, H., Li, H., Tian, T., Huang, X., Wang, L., Zhu, J., Song, L.: Adversarial attack on graph structured data. In: ICML 2018, pp. 1123–1132 (2018)
20. Dai, Q., Shen, X., Zhang, L., Li, Q., Wang, D.: Adversarial training methods for network embedding. In: WWW 2019, pp. 329–339 (2019)
21. Dehmamy, N., Barabási, A., Yu, R.: Understanding the representation power of graph neural networks in learning graph topology. In: NeurIPS 2019, pp. 15387–15397 (2019)
22. Du, T., Ji, S., Shen, L., Zhang, Y., Li, J., Shi, J., Fang, C., Yin, J., Beyah, R., Wang, T.: Cert-rnn: Towards certifying the robustness of recurrent neural networks. In: CCS 2021, pp. 516–534 (2021)
23. Feng, F., He, X., Tang, J., Chua, T.: Graph adversarial training: Dynamically regularizing based on graph structure. *IEEE Trans. Knowl. Data Eng.* **33**(6), 2493–2504 (2021)
24. Fey, M., Lenssen, J.E.: Fast graph representation learning with PyTorch geometric. *CoRR* **abs/1903.02428** (2019)
25. Gao, C., Yin, S., Wang, H., Wang, Z., Du, Z., Li, X.: Medical-knowledge-based graph neural network for medication combination prediction. *IEEE Trans. Neural Networks Learn. Syst.* **35**(10), 13246–13257 (2024)
26. Geisler, S., Schmidt, T., Sirin, H., Zügner, D., Bojchevski, A., Günnemann, S.: Robustness of graph neural networks at scale. In: NeurIPS 2021 (2021)
27. Gilmer, J., Schoenholz, S.S., Riley, P.F., Vinyals, O., Dahl, G.E.: Neural message passing for quantum chemistry. In: ICML 2017, pp. 1263–1272 (2017)
28. Gosch, L., Geisler, S., Sturm, D., Charpentier, B., Zügner, D., Günnemann, S.: Adversarial training for graph neural networks: Pitfalls, solutions, and new directions. In: NeurIPS 2023 (2023)
29. Haghshenas, S.H., Hasnat, A., Naeini, M.: A temporal graph neural network for cyber attack detection and localization in smart grids. In: ISGT 2023, pp. 1–5 (2023)
30. Hamilton, W.L., Ying, Z., Leskovec, J.: Inductive representation learning on large graphs. In: NeurIPS 2017, pp. 1024–1034 (2017)
31. Hojny, C., Zhang, S., Campos, J.S., Misener, R.: Verifying message-passing neural networks via topology-based bounds tightening. In: ICML 2024 (2024)
32. Huang, X., Kwiatkowska, M., Wang, S., Wu, M.: Safety verification of deep neural networks. In: CAV 2017, pp. 3–29 (2017)

33. Jha, K., Saha, S., Singh, H.: Prediction of protein–protein interaction using graph neural networks. *Scientific Reports* **12**(1), 8360 (2022)
34. Jin, H., Shi, Z., Peruri, V.J.S.A., Zhang, X.: Certified robustness of graph convolution networks for graph classification under topological attacks. In: *NeurIPS 2020* (2020)
35. Katz, G., Barrett, C.W., Dill, D.L., Julian, K., Kochenderfer, M.J.: Reluplex: An efficient SMT solver for verifying deep neural networks. In: *CAV 2017*, pp. 97–117 (2017)
36. Kipf, T.N., Welling, M.: Semi-supervised classification with graph convolutional networks. In: *ICLR 2017* (2017)
37. Ko, C., Lyu, Z., Weng, L., Daniel, L., Wong, N., Lin, D.: POPQORN: quantifying robustness of recurrent neural networks. In: *ICML 2019*, pp. 3468–3477 (2019)
38. Ladner, T., Eichelbeck, M., Althoff, M.: Formal verification of graph convolutional networks with uncertain node features and uncertain graph structure. *Trans. Mach. Learn. Res.* **2025** (2025)
39. Lai, Y., Zhu, Y., Pan, B., Zhou, K.: Node-aware bi-smoothing: Certified robustness against graph injection attacks. In: *IEEE SP 2024*, pp. 2958–2976 (2024)
40. Li, J., Peng, J., Chen, L., Zheng, Z., Liang, T., Ling, Q.: Spectral adversarial training for robust graph neural network. *IEEE Trans. Knowl. Data Eng.* **35**(9), 9240–9253 (2023)
41. Li, J., Xie, T., Chen, L., Xie, F., He, X., Zheng, Z.: Adversarial attack on large scale graph. *IEEE Trans. Knowl. Data Eng.* **35**(1), 82–95 (2023)
42. Li, M.M., Huang, K., Zitnik, M.: Graph representation learning in biomedicine and healthcare. *Nature Biomedical Engineering* **6**(12), 1353–1369 (2022)
43. Lu, C., Tan, T., Benedikt, M.: Robustness verification of graph neural networks via lightweight satisfiability testing. *CoRR* **abs/2510.18591** (2025)
44. Lu, J., Kumar, M.P.: Neural network branching for neural network verification. In: *ICLR 2020* (2020)
45. McAuley, J.J., Leskovec, J.: From amateurs to connoisseurs: modeling the evolution of user expertise through online reviews. In: *WWW 2013*, pp. 897–908 (2013)
46. Morris, C., Kriege, N.M., Bause, F., Kersting, K., Mutzel, P., Neumann, M.: TUDataset: A collection of benchmark datasets for learning with graphs. In: *ICML 2020 Workshop on Graph Representation Learning and Beyond* (2020)
47. Motie, S., Raahemi, B.: Financial fraud detection using graph neural networks: A systematic review. *Expert Syst. Appl.* **240**, 122156 (2024)
48. Mu, J., Wang, B., Li, Q., Sun, K., Xu, M., Liu, Z.: A hard label black-box adversarial attack against graph neural networks. In: *CCS 2021*, pp. 108–125 (2021)
49. Nunn, P., Sälzer, M., Schwarzentruber, F., Troquard, N.: A logic for reasoning about aggregate-combine graph neural networks. In: *IJCAI 2024*, pp. 3532–3540 (2024)
50. Osselin, P., Kenlay, H., Dong, X.: Structure-aware robustness certificates for graph classification. In: *UAI 2023*, pp. 1596–1605 (2023)
51. Rayana, S., Akoglu, L.: Collective opinion spam detection: Bridging review networks and metadata. In: *KDD 2015*, pp. 985–994 (2015)
52. Reiser, P., Neubert, M., Eberhard, A., Torresi, L., Zhou, C., Shao, C., Metni, H., van Hoesel, C., Schopmans, H., Sommer, T., Friederich, P.: Graph neural networks for materials science and chemistry. *Communications Materials* **3**(1), 93 (2022)
53. Rosenbluth, E., Tönshoff, J., Grohe, M.: Some might say all you need is sum. In: *IJCAI 2023*, pp. 4172–4179 (2023)
54. Rossi, F., Van Beek, P., Walsh, T.: *Handbook of Constraint Programming*. Elsevier (2006)
55. Salman, H., Yang, G., Zhang, H., Hsieh, C., Zhang, P.: A convex relaxation barrier to tight robustness verification of neural networks. In: *NeurIPS 2019*, pp. 9832–9842 (2019)
56. Sälzer, M., Lange, M.: Fundamental limits in formal verification of message-passing neural networks. In: *ICLR 2023* (2023)
57. Scholten, Y., Schuchardt, J., Geisler, S., Bojchevski, A., Günnemann, S.: Randomized message-interception smoothing: Gray-box certificates for graph neural networks. In: *NeurIPS 2022* (2022)
58. Schönherr, M., Lutz, C.: Logical characterizations of gnns with mean aggregation (2025), URL <https://arxiv.org/abs/2507.18145>
59. Sen, P., Namata, G., Bilgic, M., Getoor, L., Gallagher, B., Eliassi-Rad, T.: Collective classification in network data. *AI Mag.* **29**(3), 93–106 (2008)
60. Shi, Z., Zhang, H., Chang, K., Huang, M., Hsieh, C.: Robustness verification for transformers. In: *ICLR 2020* (2020)

61. Tao, S., Cao, Q., Shen, H., Huang, J., Wu, Y., Cheng, X.: Single node injection attack against graph neural networks. In: CIKM 2021, pp. 1794–1803 (2021)
62. Tjeng, V., Xiao, K.Y., Tedrake, R.: Evaluating robustness of neural networks with mixed integer programming. In: ICLR 2019 (2019)
63. Tran, H., Bak, S., Xiang, W., Johnson, T.T.: Verification of deep convolutional neural networks using imagestars. In: CAV 2020, pp. 18–42 (2020)
64. Wang, B., Jia, J., Cao, X., Gong, N.Z.: Certified robustness of graph neural networks against adversarial structural perturbation. In: KDD 2021, pp. 1645–1653 (2021)
65. Wang, D., Qi, Y., Lin, J., Cui, P., Jia, Q., Wang, Z., Fang, Y., Yu, Q., Zhou, J., Yang, S.: A semi-supervised graph attentive network for financial fraud detection. In: ICDM 2019, pp. 598–607 (2019)
66. Wang, S., Pei, K., Whitehouse, J., Yang, J., Jana, S.: Efficient formal safety analysis of neural networks. In: NeurIPS 2018, pp. 6369–6379 (2018)
67. Weng, T., Zhang, H., Chen, H., Song, Z., Hsieh, C., Daniel, L., Boning, D.S., Dhillon, I.S.: Towards fast computation of certified robustness for relu networks. In: ICML 2018, pp. 5273–5282 (2018)
68. Wu, H., Wang, C., Tyshtetskiy, Y., Docherty, A., Lu, K., Zhu, L.: Adversarial examples for graph data: Deep insights into attack and defense. In: IJCAI 2019, pp. 4816–4823 (2019)
69. Xia, Z., Yang, H., Wang, B., Jia, J.: GNNCert: Deterministic certification of graph neural networks against adversarial perturbations. In: ICLR 2024 (2024)
70. Xu, K., Chen, H., Liu, S., Chen, P., Weng, T., Hong, M., Lin, X.: Topology attack and defense for graph neural networks: An optimization perspective. In: IJCAI 2019, pp. 3961–3967 (2019)
71. Xu, K., Hu, W., Leskovec, J., Jegelka, S.: How powerful are graph neural networks? In: ICLR 2019 (2019)
72. Xu, K., Shi, Z., Zhang, H., Wang, Y., Chang, K., Huang, M., Kailkhura, B., Lin, X., Hsieh, C.: Automatic perturbation analysis for scalable certified robustness and beyond. In: NeurIPS 2020 (2020)
73. Ying, R., He, R., Chen, K., Eksombatchai, P., Hamilton, W.L., Leskovec, J.: Graph convolutional neural networks for web-scale recommender systems. In: KDD 2018, pp. 974–983 (2018)
74. Zhang, H., Weng, T., Chen, P., Hsieh, C., Daniel, L.: Efficient neural network robustness certification with general activation functions. In: NeurIPS 2018, pp. 4944–4953 (2018)
75. Zhang, S., Campos, J.S., Feldmann, C., Walz, D., Sandfort, F., Mathea, M., Tsay, C., Misener, R.: Optimizing over trained gnns via symmetry breaking. In: NeurIPS 2023 (2023)
76. Zhang, X., Zitnik, M.: GNNGuard: Defending graph neural networks against adversarial attacks. In: NeurIPS 2020 (2020)
77. Zhang, Z., Jia, J., Wang, B., Gong, N.Z.: Backdoor attacks to graph neural networks. In: SACMAT 2021, pp. 15–26 (2021)
78. Zhou, K., Michalak, T.P., Waniek, M., Rahwan, T., Vorobeychik, Y.: Attacking similarity-based link prediction in social networks. In: AAMAS 2019, pp. 305–313 (2019)
79. Zou, X., Zheng, Q., Dong, Y., Guan, X., Kharlamov, E., Lu, J., Tang, J.: TDGIA: effective injection attacks on graph neural networks. In: KDD 2021, pp. 2461–2471 (2021)
80. Zügner, D., Akbarnejad, A., Günnemann, S.: Adversarial attacks on neural networks for graph data. In: KDD 2018, pp. 2847–2856 (2018)
81. Zügner, D., Günnemann, S.: Adversarial attacks on graph neural networks via meta learning. In: ICLR 2019 (2019)
82. Zügner, D., Günnemann, S.: Certifiable robustness and robust training for graph convolutional networks. In: KDD 2019, pp. 246–256 (2019)
83. Zügner, D., Günnemann, S.: Certifiable robustness of graph convolutional networks under structure perturbations. In: KDD 2020, pp. 1656–1665 (2020)

A Variant for Graph Classification

For graph-classification GNNs, the process to compute the embedding vectors is the same as for node-classification GNNs, as shown in Eq. (1) in the main paper. The difference arises from how the predicted class is obtained, namely for graph classification we have:

$$\hat{c}_G = \arg \max_{c \in C} \left(\text{Softmax} \left(\mathbf{W}_3 \cdot \sum_{v \in V} \mathbf{h}_v^{(K)} + \mathbf{b}_2 \right) [c] \right), \quad (14)$$

where \mathbf{W}_3 is a learnable parameter matrix with dimension $m \times d_K$ and \mathbf{b}_2 is a learnable parameter vector.

A graph-classification GNN f is called adversarially robust if and only if, for every perturbed graph $\tilde{G} \in \mathcal{Q}(G)$, it holds that $f(\tilde{G}) = \hat{c}_G$.

Our method adapts to graph classification by simply making slight modifications to the last part of the CSP encoding to align with the operation in Eq. (14), which includes a summation of all the node embeddings and a linear transformation. We remark that our bound tightening strategies are compatible with the modified encoding. Moreover, our incremental solving-based verification can also be used with minor modification as shown in Algorithm 1. Although graph classification requires encoding of all the nodes in the graph, resulting in the same number of nodes in each GNN layer, our algorithm only encodes variables associated with the $(K - k)$ -th to K -th GNN layers in k -th iteration, which can also reduces encoding costs and enhances efficiency.

B Greedy algorithm for mean aggregation function

We focus on the upper bounds and non-corner cases; the lower bounds can be handled analogously. Recall that for the mean aggregation function,

$$\bar{z} = \max_{\substack{s_2 + s_3 \leq s \\ 0 \leq s_2 \leq |X_2| \\ 0 \leq s_3 \leq |X_3|}} \bar{z}_{s_2, s_3},$$

where

$$\begin{aligned} \bar{z}_{s_2, s_3} &= \bar{w}_{s_2, s_3} / n_{s_2, s_3}, \\ n_{s_2, s_3} &= |X_1| + |X_2| - s_2 + s_3, \\ \bar{w}_{s_2, s_3} &= \sum_{x \in X_1} \bar{x} + \sum_{1 \leq i \leq |X_2| - s_2} h_i(X_2, i) + \sum_{1 \leq i \leq s_3} h_i(X_3, i). \end{aligned}$$

For every $0 \leq i \leq |X_2|$ and $0 \leq j \leq |X_3|$, $\bar{z}_{i, j+1}$ can be rewritten as the weighted average of $\bar{z}_{i, j}$ and $h_i(X_3, j+1)$,

$$\bar{z}_{i, j+1} = \frac{(|X_1| + |X_2| - i + j) \cdot \bar{z}_{i, j} + h_i(X_3, j+1)}{|X_1| + |X_2| - i + j + 1}.$$

We first prove that the sequence $\bar{z}_{i, 0}, \bar{z}_{i, 1}, \dots, \bar{z}_{i, |X_3|}$ is *unimodal with a possible plateau*. It is sufficient to prove that the sequence satisfies the following two properties:

1. For every $0 \leq j \leq |X_3| - 2$, if $\bar{z}_{i, j+1} \leq \bar{z}_{i, j}$, then $\bar{z}_{i, j+2} \leq \bar{z}_{i, j+1}$.
2. For every $0 \leq j \leq |X_3| - 2$, if $\bar{z}_{i, j+1} < \bar{z}_{i, j}$, then $\bar{z}_{i, j+2} < \bar{z}_{i, j+1}$.

Proof. We prove the two properties as follows:

1. By the property of weighted averages, we have

$$h_i(X_3, j+1) \leq \bar{z}_{i, j+1} \leq \bar{z}_{i, j}.$$

By definition of $h_i(X_3, i)$, it follows that

$$h_i(X_3, j+2) \leq h_i(X_3, j+1).$$

Combining both inequalities gives

$$hi(X_3, j+2) \leq \bar{z}_{i,j+1}.$$

The desired property follows since $\bar{z}_{i,j+2}$ is the weighted average of $\bar{z}_{i,j+1}$ and $hi(X_3, j+2)$:

$$hi(X_3, j+2) \leq \bar{z}_{i,j+2} \leq \bar{z}_{i,j+1}.$$

2. Since $\bar{z}_{i,j+1} \neq \bar{z}_{i,j}$, it follows that $\bar{z}_{i,j+1} \neq hi(X_3, j+1)$. Therefore, the inequality between $hi(X_3, j+1)$ and $\bar{z}_{i,j+1}$ is strict, and the desired property follows by the same reasoning as above. \square

Next, note that \bar{z} can be rewritten as

$$\bar{z} = \max_{0 \leq s_2 \leq |X_2|} \left(\max_{0 \leq s_3 \leq \max(s-s_2, |X_3|)} \bar{z}_{s_2, s_3} \right).$$

Since the inner sequence is unimodal with a possible plateau, the inner maximum can be found using ternary search in $O(\log s)$ time. Hence, the total time complexity to compute \bar{z} is $O(s \log s)$.

C Proof of the Tightness of Bounds

Recall the problem:

Given three finite sets of variables X_1 , X_2 , and X_3 , the upper and lower bounds for each variable, and a non-negative integer s , compute the upper and lower bounds for the variable

$$z := \mathbf{aggr}(X_1 \cup X'_2 \cup X'_3),$$

where $\mathbf{aggr} \in \{\text{sum, max, mean}\}$, $X'_2 \subseteq X_2$, $X'_3 \subseteq X_3$, and $|X_2 \setminus X'_2| + |X'_3| \leq s$.

Max aggregation. In this case, the problem is straightforward through case-by-case analysis. The only subtlety is when X_1 is empty and $s \geq |X_2|$, in which case we may have $X'_2 = X'_3 = \emptyset$ and thus $X_1 \cup X'_2 \cup X'_3 = \emptyset$, which implies that the corresponding upper and lower bounds are 0. Therefore, we must take 0 into consideration.

Mean aggregation. In this case, recall that we reduce the original problem to a combination of subproblems. For non-negative integers s_2 and s_3 , define the variable

$$z_{s_2, s_3} := \mathbf{mean}(X_1 \cup X'_2 \cup X'_3),$$

where $X'_2 \subseteq X_2$, $X'_3 \subseteq X_3$, $|X_2 \setminus X'_2| = s_2$, and $|X'_3| = s_3$. The upper and lower bounds of the original problem z are given by

$$\bar{z} = \max_{\substack{s_2+s_3 \leq s \\ 0 \leq s_2 \leq |X_2| \\ 0 \leq s_3 \leq |X_3|}} \bar{z}_{s_2, s_3} \quad \text{and} \quad \underline{z} = \min_{\substack{s_2+s_3 \leq s \\ 0 \leq s_2 \leq |X_2| \\ 0 \leq s_3 \leq |X_3|}} \underline{z}_{s_2, s_3}. \quad (15)$$

Note that Eq. (15) covers all possible allocations of budgets (s_2, s_3) such that $s_2 + s_3 \leq s$. The correctness of this reduction is obvious.

Next, we show that the upper and lower bounds of the variable z_{s_2, s_3} can be computed efficiently. Here we focus on the upper bound; a similar argument applies to the lower bound.

Let (s_2, s_3) be a fixed pair of non-negative integers satisfying $s_2 + s_3 \leq s$, $0 \leq s_2 \leq |X_2|$, and $0 \leq s_3 \leq |X_3|$. Let

$$\begin{aligned} n_{s_2, s_3} &:= |X_1| + |X'_2| + |X'_3| \\ &= |X_1| + |X_2| - s_2 + s_3. \end{aligned}$$

Note that

$$\begin{aligned}
z_{s_2, s_3} &= \mathbf{mean}(X_1 \cup X'_2 \cup X'_3) \\
&= \frac{1}{n_{s_2, s_3}} \cdot \mathbf{sum}(X_1 \cup X'_2 \cup X'_3) \\
&= \frac{1}{n_{s_2, s_3}} \cdot (\mathbf{sum}(X_1) + \mathbf{sum}(X'_2) + \mathbf{sum}(X'_3)).
\end{aligned}$$

Because the values of s_2 and s_3 are fixed, the selections of $X'_2 \subseteq X_2$ and $X'_3 \subseteq X_3$ are independent. Thus, the upper bound of z_{s_2, s_3} is given by the sum of upper bounds of $\mathbf{sum}(X_1)$, $\mathbf{sum}(X'_2)$, and $\mathbf{sum}(X'_3)$, divided by n_{s_2, s_3} where $X'_2 \subseteq X_2$, $X'_3 \subseteq X_3$, $|X_2 \setminus X'_2| = s_2$, and $|X'_3| = s_3$.

Observe that, for a set of variables Y , because the sum function is monotonic w.r.t. each variable, the upper bound of the sum of the set Y is given by the sum of the upper bounds of the variables in Y . Therefore, we have the following conclusions:

- The upper bound of $\mathbf{sum}(X_1)$ is $\sum_{x \in X_1} \bar{x}$.
- For $\mathbf{sum}(X'_2)$ where $X'_2 \subseteq X_2$ and $|X_2 \setminus X'_2| = s_2$. Since $|X'_2| = |X_2| - s_2$, the upper bound of $\mathbf{sum}(X'_2)$ is given by the sum of the $(|X_2| - s_2)$ -largest upper bounds in X_2 , that is, $\sum_{1 \leq i \leq |X_2| - s_2} \bar{h}(X_2, i)$.
- Similarly, since $X'_3 \subseteq X_3$ and $|X'_3| = s_3$, the upper bound of $\mathbf{sum}(X'_3)$ is $\sum_{1 \leq i \leq s_3} \bar{h}(X_3, i)$.

Thus \bar{z}_{s_2, s_3} is upper bounded by

$$\frac{1}{n_{s_2, s_3}} \left(\sum_{x \in X_1} \bar{x} + \sum_{1 \leq i \leq |X_2| - s_2} \bar{h}(X_2, i) + \sum_{1 \leq i \leq s_3} \bar{h}(X_3, i) \right).$$

Note that the bound is tight. That is, there exist sets $X'_2 \subseteq X_2$ and $X'_3 \subseteq X_3$ with $|X_2 \setminus X'_2| = s_2$ and $|X'_3| = s_3$ that achieve this bound exactly.

D Proof of Theorem 2

Recall the theorem:

Given a GNN f , an attributed directed graph G , and a perturbation space $\mathcal{Q}(G)$, f is adversarially robust (for a node t , if it is a node-classification GNN) if and only if Algorithm 1 returns **robust**.

Proof. For $1 \leq k \leq K$, let $\Phi_k := \varphi_{obj} \wedge \bigwedge_{1 \leq i \leq k} \varphi_i$. Recall that φ_k is the encoding of the computation of the k -th layer of the GNN f . Following the intuition described in Section 4.1, it is straightforward to show that f is adversarially robust for t if and only if Φ_K is unsatisfiable.

If Algorithm 1 returns **nonrobust**, then Φ_K is satisfiable. Hence, f is not adversarially robust (for node t).

On the other hand, observe that for $1 \leq k \leq K$,

$$\Phi_K = \Phi_k \wedge \bigwedge_{k < i \leq K} \varphi_i.$$

If f is not adversarially robust (for node t), then Φ_K is satisfiable, which implies that Φ_k is also satisfiable for $1 \leq k \leq K$. Therefore, Algorithm 1 returns **nonrobust**. \square

E Model Implementation and Training

Implementation. To evaluate the performance of verifiers, we implemented a batch of GraphSAGE models built using PyTorch and the SAGEConv module of PyTorch Geometric. The aggregation function of SAGEConv was configured as sum, max, and mean, respectively, to build distinct models. The models consist of 3 SAGEConv layers (i.e., $K = 3$), with input dimension being the dimension of attributes, all hidden layers having a dimension of 32, and output dimension being the number of classes. For graph-classification GNNs, the final linear layer also has an input dimension of 32. Except for the last layer, the output of each layer is passed through a ReLU activation function. Finally, a Softmax function is applied to the output of the last layer to obtain predictions for each class.

Datasets. We trained models on 4 node classification datasets and 2 graph classification datasets. Cora and CiteSeer are two standard graph benchmarks that have been employed for evaluating verification algorithms in a number of previous works [5, 31, 57, 64]. Amazon and Yelp are two Internet fraud datasets, and we employed them to evaluate the performance of our algorithm on real-world high-stakes tasks. Because Amazon and Yelp are heterogeneous graphs with three types of edges, we used only the U-P-U edges for Amazon and R-U-R edges for Yelp to ensure compatibility with our GNN architectures. MUTAG and ENZYMES are two biochemical datasets to predict whether specific properties are present based on the molecular structure. Detailed information of these datasets is shown in Table 1.

Table 1: Statistical information of datasets. For graph-classification datasets, #Nodes and #Edges represent the average number of nodes and edges per graph, respectively.

Dataset	#Graphs	#Nodes	#Edges	#Attributes	#Classes
Cora	1	2,708	5,429	1,433	7
CiteSeer	1	3,312	4,715	3,703	6
Amazon	1	11,944	351,216	25	2
Yelp	1	45,954	98,630	32	2
MUTAG	188	17.9	39.6	7	2
ENZYMES	600	32.6	124.3	3	6

Training. For Cora and Citeseer, we randomly selected 30% of the nodes as the training set, 20% as the validation set, and the remaining 50% as the test set. For Amazon and Yelp, given the highly imbalanced distribution of the two classes, we randomly selected 350 (from Amazon) and 2,000 (from Yelp) nodes per class as the training set, 70 (from Amazon) and 400 (from Yelp) nodes per class as the validation set, and the remaining nodes as the test set. For MUTAG and ENZYMES, we randomly selected 80% of the graphs as the training set due to the small size of the dataset, 10% as the validation set, and the remaining 10% as the test set. All models were trained for 400 epochs with learning rate 0.001 and weight decay 5×10^{-5} , and early stopping is applied if the validation loss exceeded the average of the last 10 epochs after training for more than 200 epochs. The models have been properly trained, and the accuracy on test sets is summarised in Table 2.

Table 2: Accuracy of the trained GNN models on test sets.

aggr	Cora	CiteSeer	Amazon	Yelp	MUTAG	ENZYMES
sum	81.02%	71.68%	95.97%	79.12%	88.89%	68.33%
max	80.35%	72.40%	96.19%	79.02%	77.78%	68.33%
mean	81.39%	72.58%	97.55%	80.52%	88.89%	71.67%

F Comprehensive Experimental Results

F.1 Comparison with SCIP-MPNN

As described in Section 5.2, we compared the performance of GNNEV and SCIP-MPNN on sum-aggregated 3-layer GNNs. Table 3 shows the comprehensive comparison results under different global structural perturbation budgets Δ . The average runtime, the number of solved tasks, and the number of winning tasks (i.e., when the runtime of the current verifier is shorter than other verifier(s) on that task) for each verifier are reported for the set of all instances and the set of robust instances, respectively. Across models under different budgets, GNNEV consistently outperformed SCIP-MPNN in terms of the number of winning tasks, especially on the robust instances.

Table 3: Detailed comparison results of GNNEV and SCIP-MPNN on node (Cora, CiteSeer) and graph (MUTAG, ENZYMEs) classification for 3-layer GNNs and a range of perturbation budgets. The #Win column indicates the number of winning tasks (i.e. when the runtime of the current verifier is shorter than other verifier(s) on that task), and the larger number on the same set of instances is shown in **bold**.

Δ	SCIP-MPNN						GNNEV					
	All instances			Robust instances			All instances			Robust instances		
	Time(s)	#Solved	#Win	Time(s)	#Solved	#Win	Time(s)	#Solved	#Win	Time(s)	#Solved	#Win
<i>Cora</i>												
1	13.84	2,708	73	13.06	2,544	59	5.06	2,708	2,635	4.72	2,544	2,485
2	13.86	2,708	58	12.15	2,404	45	5.12	2,708	2,650	4.45	2,404	2,359
5	13.79	2,708	132	10.32	2,259	104	6.92	2,708	2,576	5.39	2,259	2,155
10	13.87	2,706	162	10.25	2,249	136	8.10	2,708	2,546	6.53	2,251	2,115
50	13.65	2,706	178	10.08	2,249	148	7.79	2,708	2,530	6.30	2,251	2,103
<i>CiteSeer</i>												
1	9.59	3,308	1,126	9.12	3,156	1,009	6.14	3,312	2,186	5.70	3,160	2,151
2	9.59	3,307	1,300	8.77	3,076	1,134	6.84	3,312	2,012	6.08	3,081	1,947
5	9.63	3,307	1,550	8.04	3,010	1,327	9.07	3,308	1,759	7.56	3,010	1,686
10	10.26	3,307	1,548	8.43	2,985	1,319	9.51	3,308	1,761	8.06	2,990	1,672
50	10.37	3,305	1,561	7.52	2,978	1,328	9.41	3,295	1,750	7.14	2,980	1,654
<i>MUTAG</i>												
1	31.08	188	0	0.42	6	0	3.38	188	188	0.03	6	6
2	111.60	167	37	9.68	6	0	37.93	185	148	7.12	6	6
5	193.22	106	34	5.48	4	1	57.58	148	134	4.75	4	3
10	212.52	70	19	0.00	0	0	79.37	136	130	0.00	0	0
50	193.80	98	21	0.00	0	0	81.89	136	130	0.00	0	0
<i>ENZYMEs</i>												
1	117.70	572	10	113.95	556	10	36.33	600	590	34.54	582	572
2	121.51	491	226	92.09	398	183	106.15	495	298	77.81	399	241
5	255.15	35	28	74.34	2	1	85.17	152	142	22.14	43	43
10	277.49	20	11	11.27	1	0	60.26	210	202	4.67	9	9
50	291.15	20	5	0.55	1	0	56.80	544	539	0.03	2	2

F.2 Verification Results and Performance

We evaluated the performance of GNNEV on 3-layer GNNs. Due to the large number of nodes in Amazon and Yelp, we sampled 1,000 nodes from each dataset to form the instances for verification. Initially, we selected nodes, for which the size of 3-hop incoming neighbours set was within the range $[2, 200]$ and which were correctly predicted by the model. Next, if the number of nodes in a class was less than 500, all of them were selected, and nodes in another class were uniformly sampled to make the instances up to 1,000; otherwise, 500 nodes were uniformly sampled from each class. We built two kinds of fragile edge sets. For edge deletion, we set all existing edges as fragile, i.e., $F = E$. For edge addition, we sampled a set of non-edges in each graph as fragile. Specifically, we randomly selected one and three non-edge(s) pointing to each node to build F for node- and graph-classification datasets, respectively. This ensures that there are several fragile edges for any verification task.

Results. Fig. 5,6 illustrate the runtime of GNNEV under different aggregation functions and budgets for structural perturbations (edge deletion and addition, respectively). For edge addition, GNNEV successfully solved all tasks within the time limit for Cora, Amazon, and Yelp (Fig. 6a,6c,6d). For CiteSeer, there were 2 ($\Delta = 1$), 78 ($\Delta = 5$) and 152 ($\Delta = 10$) tasks left unsolved with max aggregation, indicating that the difficulty of the problem increases with larger budgets (Fig. 6b). Since the fragile edge set F only included one non-edge for each node, the number of edges that can be perturbed in each task is much lower for edge addition, which makes the corresponding CSP easier to solve compared with edge deletion. Note that setting F to a large size can lead to a notable decrease in verification efficiency.

Fig. 7,8 show the evolution of the number of robust and nonrobust nodes verified by GNNEV as the structural perturbation budget increases. We observed that, on node-classification datasets, the robustness of mean-aggregated GNNs is significantly lower compared to other GNNs, on Cora, CiteSeer and Amazon for edge deletion, and on Amazon for edge addition. On graph-classification datasets, lack of robustness has been identified across aggregations. This indicates that GNNEV can reveal the robustness flaws of GNN models, which is beneficial for deploying these models in high-stakes applications. Furthermore, for most nodes, the transition from robust to nonrobust occurred when $\Delta \leq 3$, which also demonstrates the vulnerability of GNN models to simple adversarial attacks.

Fig. 9 shows the evaluation results of GNNEV for attribute perturbations on two node-classification fraud datasets, Amazon and Yelp, given their rich attribute information. Amazon has 25 attributes, including both continuous and discrete values. Yelp has 32 attributes, all of which are normalised to continuous values within $[0, 1]$. We performed an experiment, where we perturbed a single attribute for each run, for perturbation budget defined as the minimum to maximum values that have appeared in the data. GNNEV completed all runs within the time limit, demonstrating its efficiency. From the results on mean-aggregated GNNs, the models exhibited vulnerability on most attributes, especially on Yelp, where half of the nodes were successfully attacked by perturbing 13 out of 32 attributes.

F.3 Ablation Studies

We performed ablation experiments to evaluate the effectiveness of the proposed incremental solving algorithm. A variant of GNNEV was developed, where the incremental solving algorithm was replaced with a one-time solution of the complete encoding. We refer to this variant as GNNEV w/o IS. The experiments were conducted on structural perturbations for 3-layer GNNs, with perturbation budget $\Delta = 2$ and fragile edge set $F = E$.

The results of the ablation experiments are shown in Table 4. The number of winning tasks and the average runtime on Cora and CiteSeer are reported. Compared to its variant without incremental solving, GNNEV demonstrated lower average runtime and was more competitive on more tasks. Specifically, on robust instances, the incremental solving algorithm lowers the runtime of up to 82% of tasks (on CiteSeer, mean aggregation). These results indicate that the proposed incremental solving algorithm effectively enhances the practical performance of our exact verifier, offering the greatest advantage on robust instances, which is consistent with its design.

We have also shown the effectiveness of the proposed bound tightening strategies. Table 5 summarizes the mean and maximum gaps between the upper and lower bounds of the node embedding variables $y_{v,i}^{(k)}$ defined by Eq. (11) across 4 datasets. The experiments were conducted on 3-layer GNNs,

with perturbation budget $\Delta = 1$ and fragile edges set $F = E$. Compared with the plain method as described in Section 4.2, our tightened bounds achieved lower mean and maximum gaps for all aggregations and layers k . We remark that the sum aggregation function resulted in significantly larger gaps than mean and max, leading to performance drop of the solver.

Table 4: Ablation experiments on the incremental solving algorithm of GNNEV. The relatively better results are shown in **bold**.

Dataset	aggr	GNNEV		GNNEV w/o IS	
		#Win	Time(s)	#Win	Time(s)
<i>All instances</i>					
Cora	sum	1,743	7.84	965	9.21
	max	1,313	19.81	1,383	20.57
	mean	1,532	32.06	1,176	34.88
CiteSeer	sum	2,491	10.09	821	13.35
	max	1,989	28.47	1,222	29.82
	mean	1,759	15.15	1,553	17.41
<i>Robust instances</i>					
Cora	sum	1,467	5.02	476	6.49
	max	1,084	11.87	855	12.68
	mean	931	20.33	269	23.03
CiteSeer	sum	2,217	7.34	499	8.73
	max	1,767	7.33	778	8.72
	mean	1,257	7.75	273	10.09

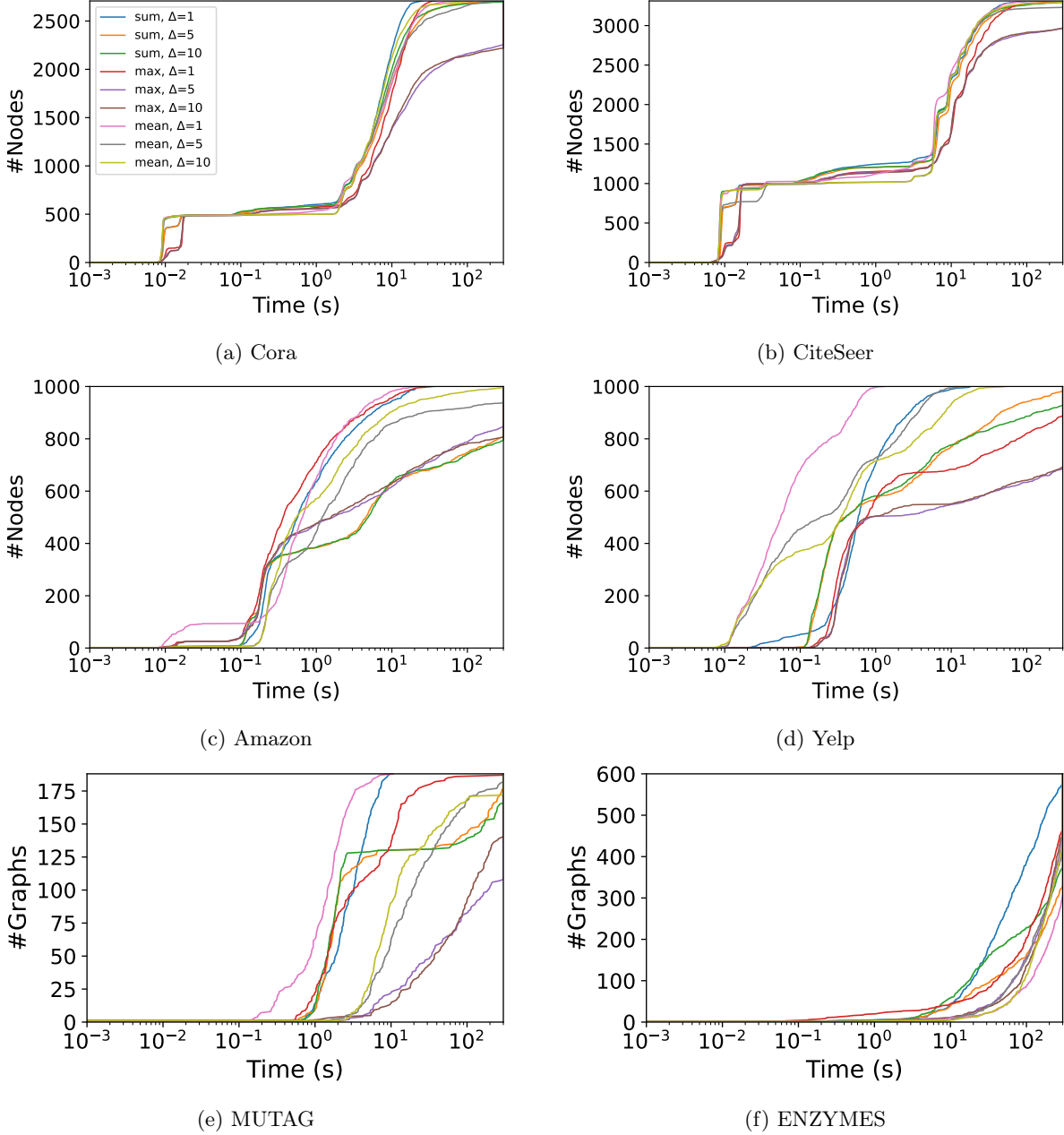


Fig. 5: The number of tasks solved by GNNEV on node classification (a-d) and graph classification (e-f) plotted against runtime under different aggregations and budgets. Only edge deletions are allowed ($F = E$). The verification objective is as defined in Section 4.1, Eq. (13).

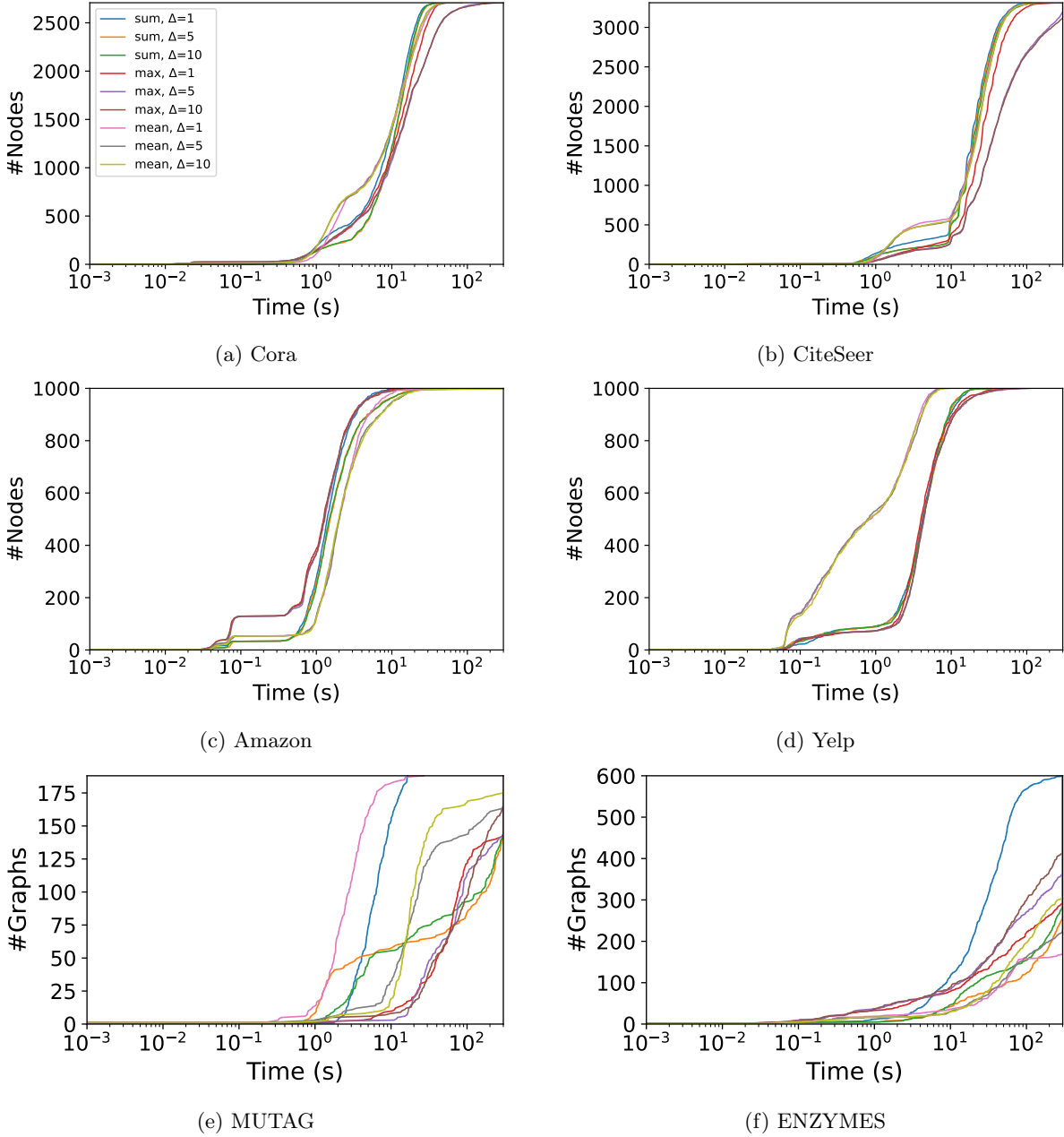


Fig. 6: The number of tasks solved by GNNEV on node classification (a-d) and graph classification (e-f) plotted against runtime under different aggregations and budgets. Only edge additions are allowed under predefined fragile non-edge sets as detailed in Appendix F.2.

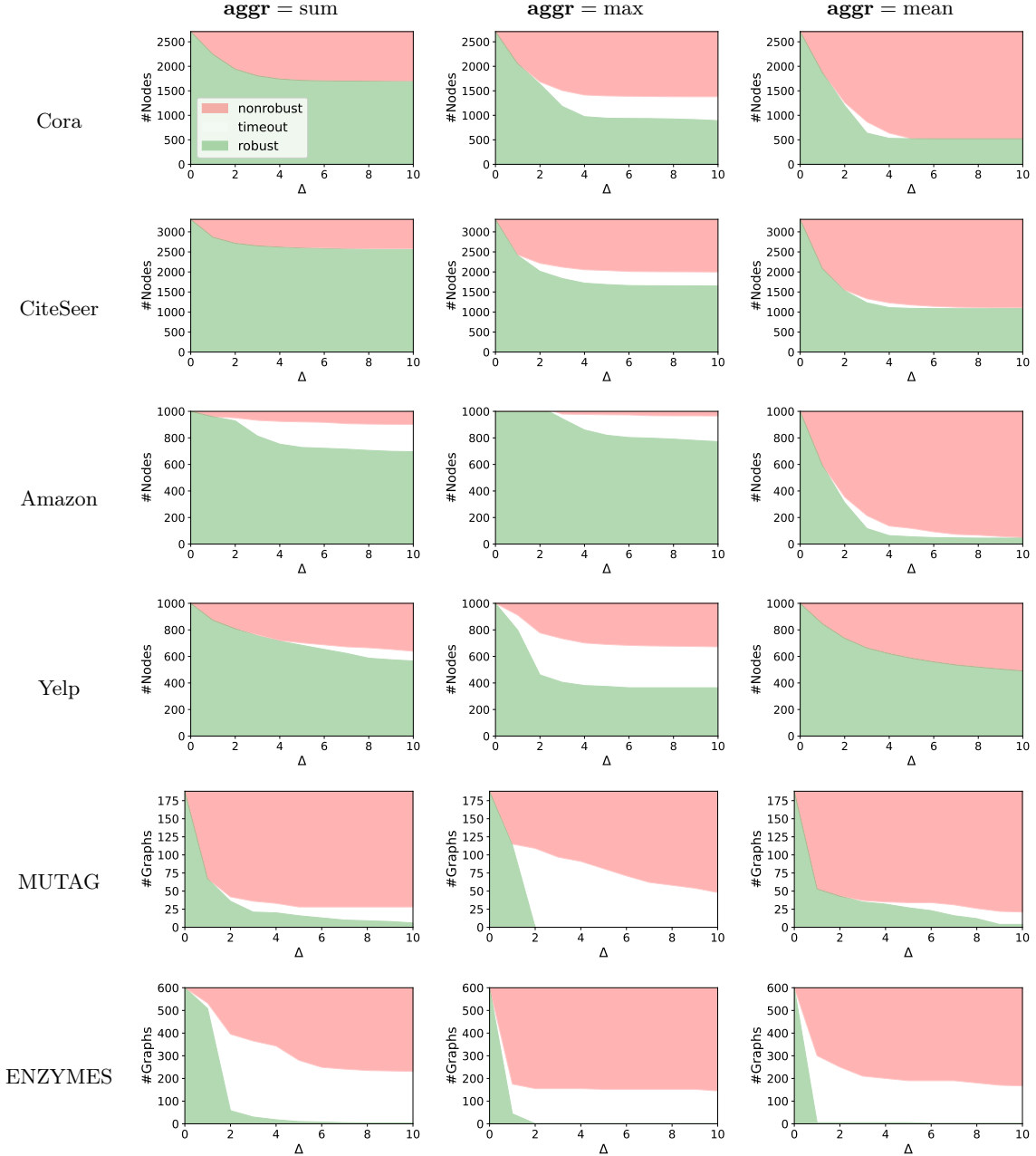


Fig. 7: The evolution of the number of robust and nonrobust nodes verified by GNNEV on node classification (top four rows) and graph classification (bottom two rows) as the global structural perturbation budget Δ increases. Only edge deletions are allowed, and all edges are set as fragile.

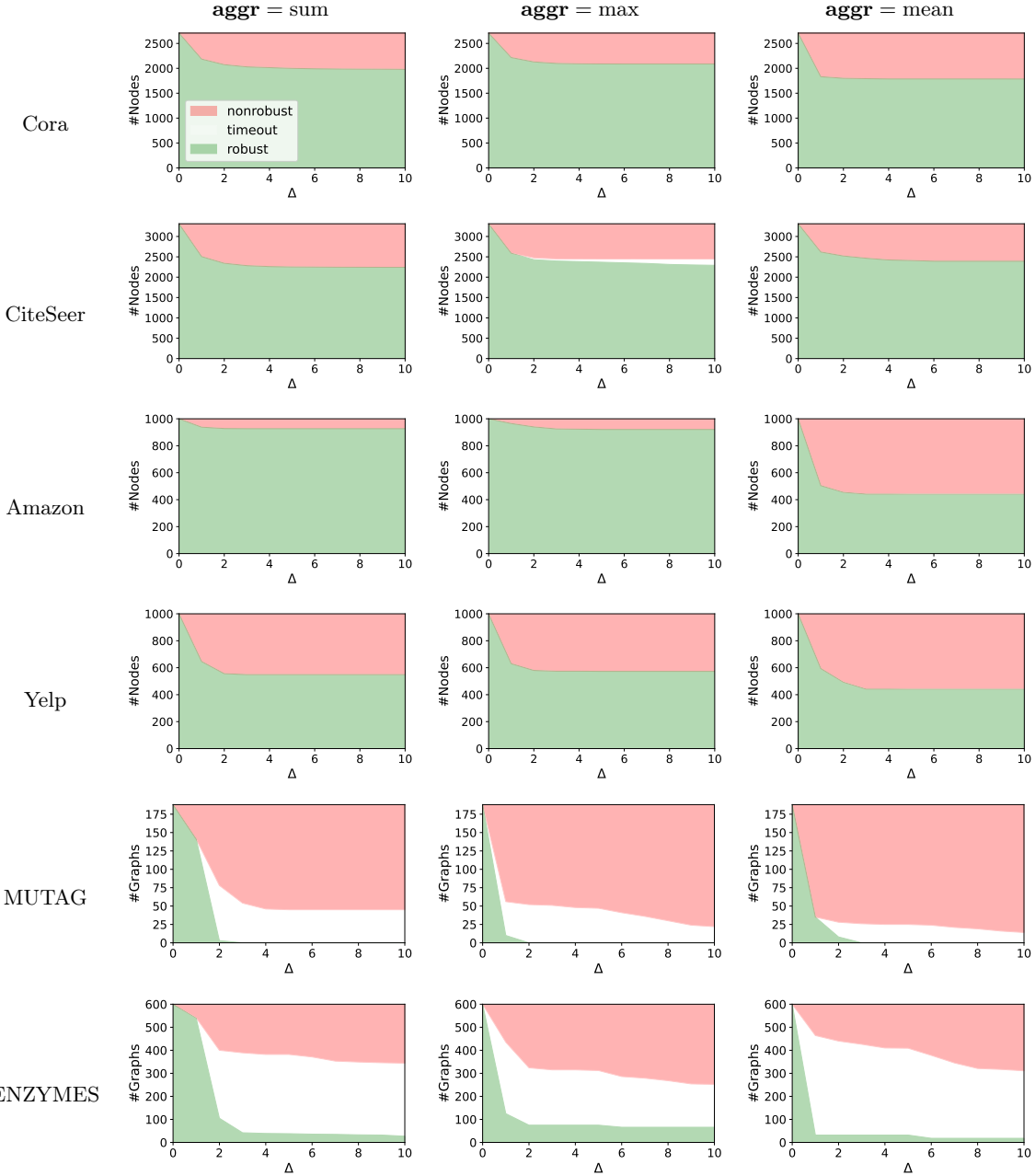


Fig. 8: The evolution of the number of robust and nonrobust nodes verified by GNNEV on node classification (top four rows) and graph classification (bottom two rows) as the global structural perturbation budget Δ increases. Only edge additions are allowed under predefined fragile non-edge sets as detailed in Appendix F.2.

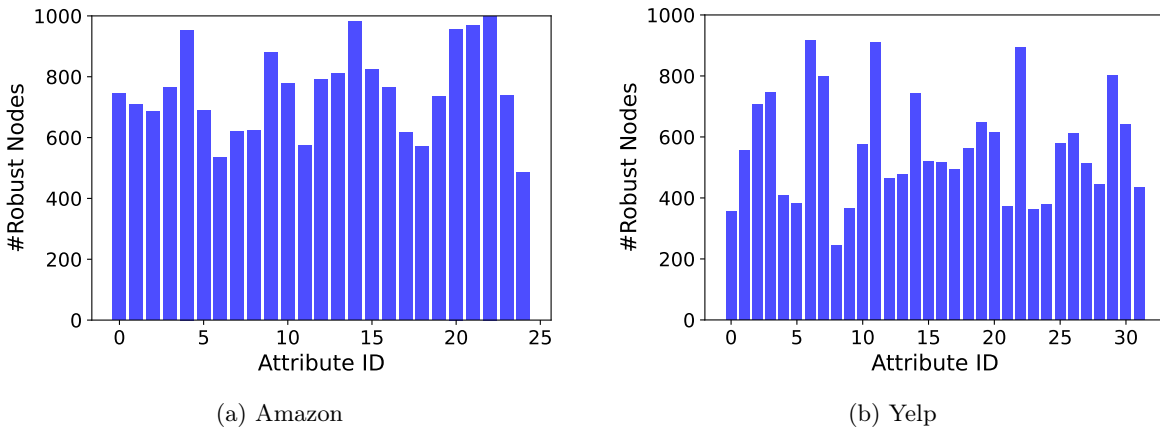


Fig. 9: The number of robust tasks solved by GNNEV on real-world node-classification datasets for mean-aggregated GNNs. Only attribute perturbations are allowed on each single dimension under budgets as detailed in Appendix F.

Table 5: Comparison of the gaps between the upper and lower bounds of node embedding variables for the tightened and plain bound propagation methods.

aggr	k	Tightened Bounds		Plain Bounds	
		Mean gap	Max gap	Mean gap	Max gap
<i>Cora</i>					
sum	1	0.58	2.66	0.67	3.42
	2	7.46	38.26	9.29	50.58
	3	91.94	472.87	104.66	566.26
max	1	0.57	3.28	0.66	3.75
	2	5.25	17.12	6.42	22.10
	3	50.94	130.73	58.00	151.40
mean	1	0.42	2.35	0.73	3.68
	2	4.17	11.82	7.30	22.83
	3	41.60	93.48	65.96	162.08
<i>CiteSeer</i>					
sum	1	0.46	6.13	0.55	14.36
	2	4.99	97.94	6.40	189.29
	3	51.57	1,002.33	59.86	1,354.72
max	1	0.46	4.00	0.53	7.41
	2	3.70	23.50	4.55	37.25
	3	32.53	144.33	37.55	198.76
mean	1	0.34	2.00	0.51	7.66
	2	2.91	10.39	4.35	38.81
	3	25.83	77.49	35.81	203.99
<i>Amazon</i>					
sum	1	46.29	993.37	144.50	21,387.24
	2	391.64	14,691.80	562.75	25,208.20
	3	2,008.59	37,071.13	2,678.37	60,287.40
max	1	40.71	991.43	74.81	1,317.29
	2	101.59	1,626.05	134.98	2,378.28
	3	525.86	4,350.96	611.23	4,819.04
mean	1	19.53	1,025.55	68.98	1,126.02
	2	54.64	1,681.41	143.64	1,921.16
	3	226.63	3,832.60	466.67	4,021.53
<i>Yelp</i>					
sum	1	1.80	6.76	11.16	182.42
	2	28.76	387.72	391.38	17,145.60
	3	711.55	34,765.66	7,880.43	993,569.36
max	1	0.66	3.69	2.37	4.51
	2	5.42	27.59	17.85	38.48
	3	111.11	205.89	191.89	280.45
mean	1	0.09	2.11	0.43	2.49
	2	0.38	5.14	2.04	6.42
	3	12.45	48.56	34.62	54.53